火山 第58巻（2013）
第2号, CD-BOOK

A1. Calderas and active volcanoes in central to eastern Hokkaido

Takeshi Hasegawa*, Mitsuhiro Nakagawa**, Hiroshi Kishimoto***

** Department of Earth Sciences, College of Science, Ibaraki University, Mito, Japan*
*** Department of Natural History Sciences, Graduate School of Science, Hokkaido University, Sapporo, Japan*
**** Department of Disaster Prevention, Asia Air Survey Company with Limited Liability, Kawasaki, Japan*

1. Introduction

Quaternary volcanoes are distributed at three distinct volcanic fields in Hokkaido: the southwest Hokkaido volcanic field (SWH V.F.), the Taisetsu-Tokachi-Shikaribetsu volcanic field (TTS V.F.) in central Hokkaido, and the Akan-Shiretoko volcanic field (AKS V.F.) in eastern Hokkaido (Figure 1). We will visit the TTS and AKS volcanic fields, which are located at the southern end of the Kuril arc. We will focus on various types of young volcanoes, a volcanic complex (the Taisetsu-Tokachi volcano group), and caldera volcanoes (Akan, Kutcharo, and Mashu), which erupted widely distributed tephra deposits. We will investigate these deposits to reconstruct the eruption sequences and magmatic processes. In addition, we will climb active volcanoes (Tokachi-dake and

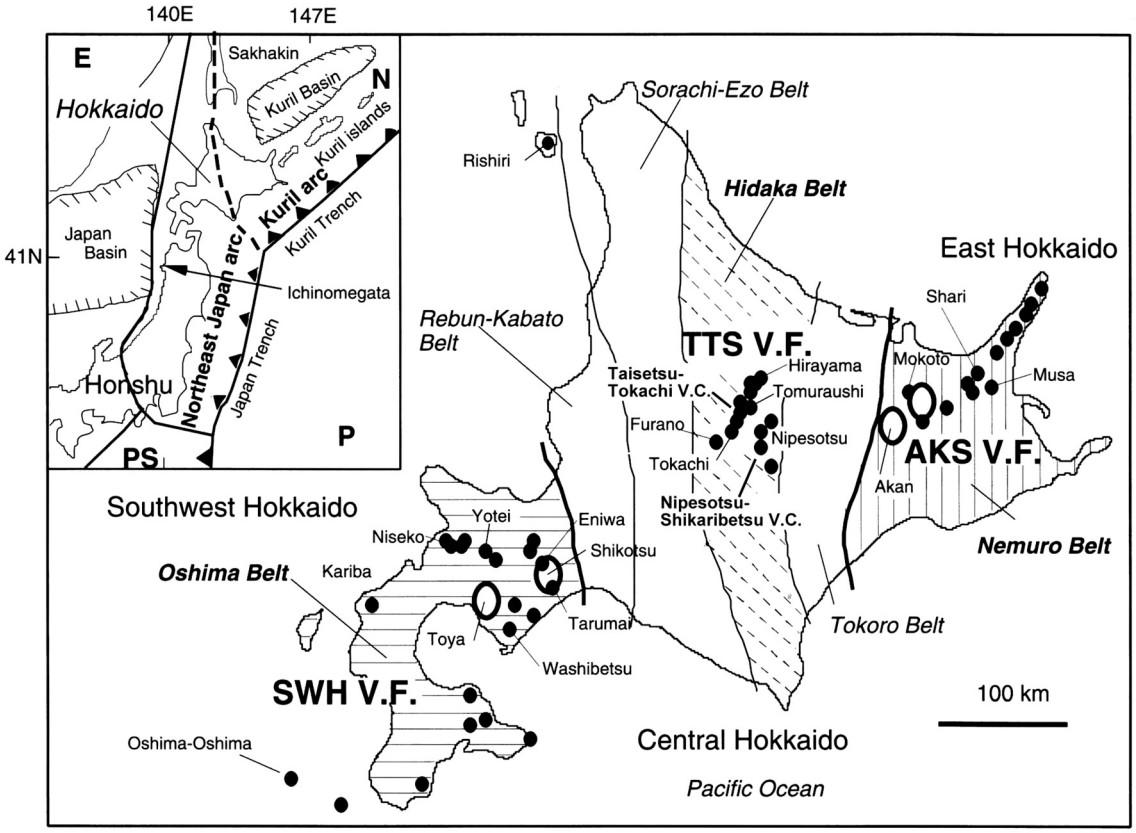

Figure 1. Distribution of Quaternary volcanoes and the tectonic setting of Hokkaido and surrounding areas (inset). The main part of the figure shows the distribution of Quaternary volcanoes (closed circles) and calderas (large open circles) in Hokkaido (based on Nakagawa et al., 1995). The Quaternary volcanoes, except for Rishiri volcano, are distributed in three volcanic fields: the southwest Hokkaido (SWH), Taisetsu-Tokachi-Shikaribetu (TTS), and Akan-Shiretoko (AKS) Quaternary volcanic fields. The italicized names are geological provinces (based on Kiminami et al., 1990). The three fields are distributed in a distinct geological province. It should be emphasized that the central Hokkaido belt (TTS) had developed along the paleo-plate boundary and that both southwestern and eastern Hokkaido are arc-trench systems characterized by open back-arc basins during the Miocene. The names of the volcanoes cited in the text (Nakagawa, 1999) are also shown. V.C.=Volcanic Chain. Inset shows the boundaries between the four plates. N, North America (or Okhotsk) plate; P, pacific plate; PS, Philippine Sea plate; E, Eurasia plate. The boundary between the North American and Eurasia plates has been situated west of Hokkaido since the Quaternary (the broken line indicates the previous boundary location).

Me-Akan) to observe their respective structures.

This paper is composed of five chapters. In the next Chapter 2 and 3, general background of tectonics and magmatism for whole of Hokkaido are described. In Chapter 4, Quaternary volcanism of central Hokkaido are summarized, especially focusing on Tokachi-dake volcano. In Chapter 5, tephro-startigraphy and petrology of three Quaternary caldera volcanoes in eastern Hokkadio (Akan, Kutcharo, Mashu) are presented. In addition, descriptions of outcrops in this field trip are addressed in another chapter.

2. Tectonic setting and Cenozoic volcanism in Hokkaido

Hokkaido is located at the junction of two arc-trench systems, the northeast Japan (NE Japan) and Kuril arcs (Figure 2). Several striking tectonic events have occurred in and around Hokkaido. During the Cretaceous, the triple junction between the Pacific, North America, and Eurasia plates was located south of Hokkaido, and the boundary between the North America and Eurasia plates was situated from central Hokkaido to Sakhalin (Chapman and Solomon, 1976). The Pacific plate has been subducting beneath the North America and Eurasia plates since that time. Two back-arc basins, the Japan and Kuril basins, were forming until the middle Miocene (Tamaki, 1995; Gnibidenko et al., 1995). Subsequently, the Kuril fore-arc sliver has been moving westward since the late Miocene, colliding with the NE Japan arc, due to the oblique subduction of the Pacific plate (Kimura, 1986). According to the locations of earthquakes, the present plate boundary between the North America (or Okhotsk) and Eurasia plates is considered to be located along the eastern rim of the Japan Sea (Nakamura, 1983). Thus, the plate boundary had jumped from central Hokkaido and Sakhalin after the late Miocene. However, the timing of the jump and the mode of tectonics along the plate boundary are still ambiguous. At present, Hokkaido island is situated on the North America plate (or Okhotsk microplate), and the Pacific plate is subducting beneath the island along the Japan and Kuril trenches.

The above tectonic events reflected Neogene volcanism in Hokkaido. Nakagawa et

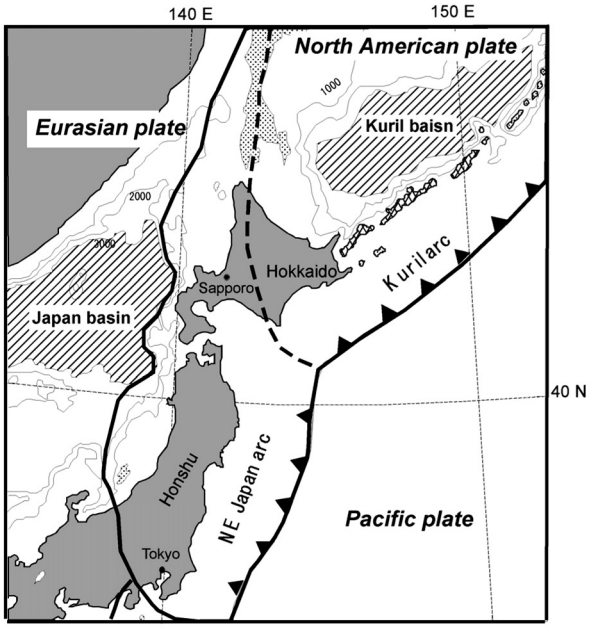

Figure 2. Tectonic setting around Hokkaido. The previous (dotted line) and newly recognized (solid line) plate boundaries are based on Chapman and Solomon (1976) and Seno (1985), respectively.

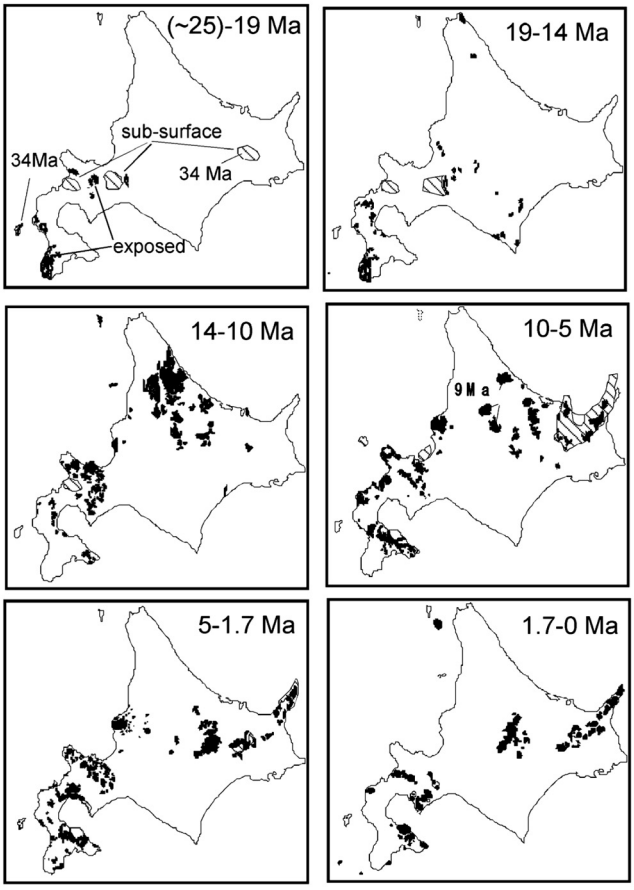

Figure 3. Temporal and spatial changes in volcanism (black and hatched areas) since around 20 Ma (Nakagawa et al., 1995; Hirose and Nakagawa, 1999; Hirose et al., 2000).

al. (1995), Hirose and Nakagawa (1999), and Hirose et al. (2000) showed spatial and temporal variations in volcanism since ~20 Ma (Figure 3) to discuss the relationships between tectonic movement and volcanism. These studies also revealed geochemical features of the volcanic rocks and concluded that subduction-related volcanism has continued since ~12 Ma in west Hokkaido and since ~14 Ma in east Hokkaido. This arc volcanism since the late Miocene has changed the volcanic fields in Hokkaido. Relatively extensive volcanism during the Pliocene converged into three volcanic fields and the isolated Rishiri volcano in the Quaternary. There are no Quaternary volcanoes between these volcanic fields.

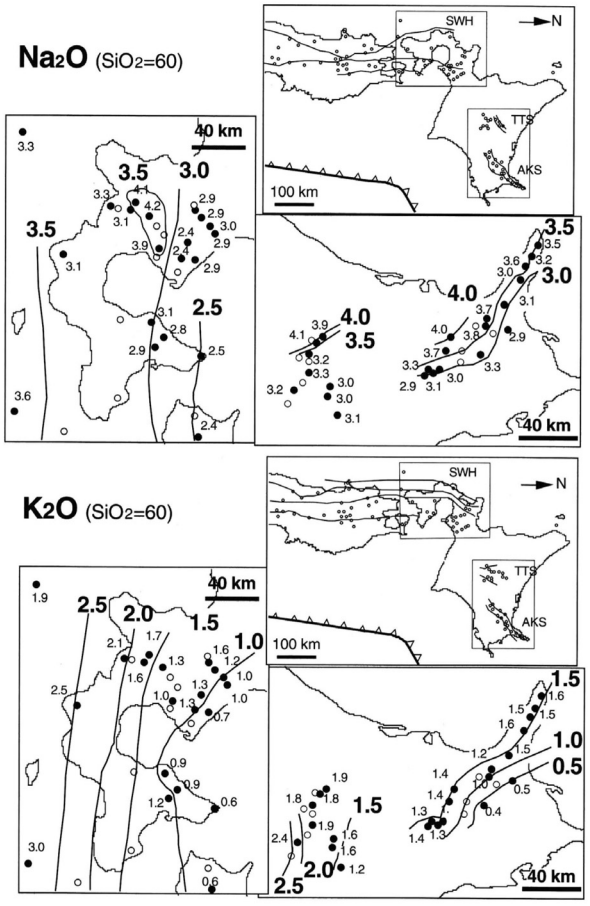

Figure 4. Spatial variations in SiO_2-normalized K_2O and Na_2O values in Hokkaido. Least squares calculations of andesite samples with SiO_2=56-64 (water-free and 100% normalized value) were used to determine the SiO_2-normalized values of basaltic to dacitic rock samples from 52 volcanoes in Hokkaido (Nakagawa et al., 1995) and 25 volcanoes in northern Honshu (Nakagawa, 1992). The geographic distributions of these volcanoes are shown on the figure.

3. Characteristics of Quaternary magmatism in Hokkaido

Nakagawa (1999) summarized the spatial compositional variations of Quaternary

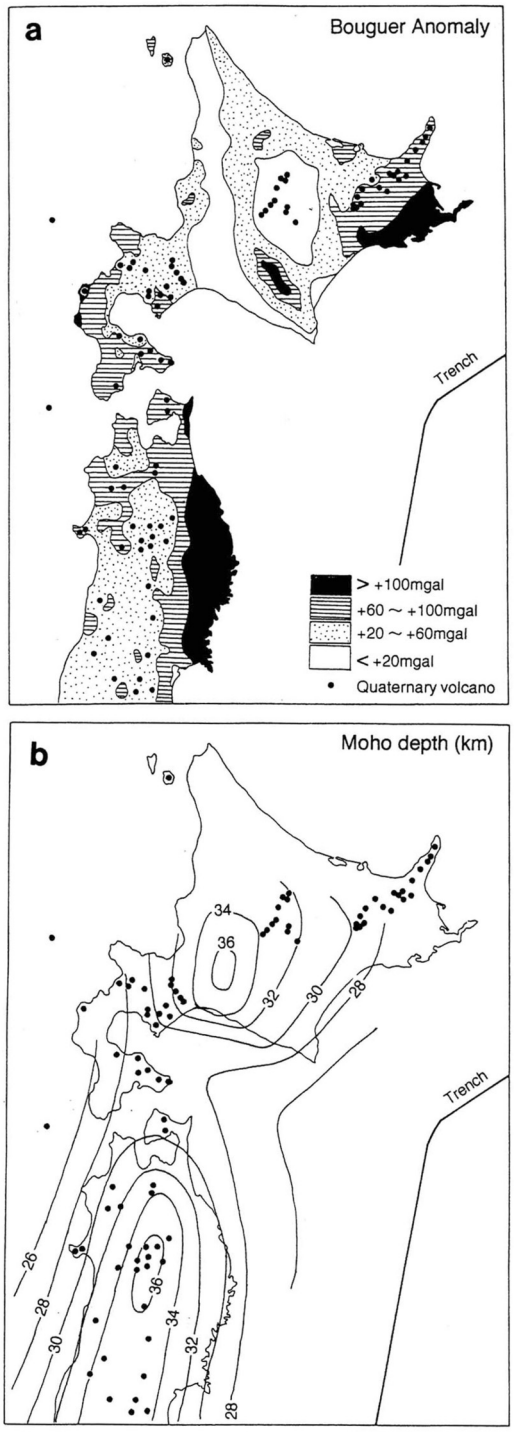

Figure 5. (a) Map showing the contoured Bouguer anomalies modified from Kono and Flu-use (1989). Filled circles indicate the Quaternary volcanic centers. The TTS field is located in the negative Bouguer anomaly area (< 20 mgal), whereas the SWH and AKS fields occur within positive Bouguer anomaly areas (20 mgal <). (b) Map showing the contours of Moho depths (based on Zhao et a1., 1992) and the volcanic centers (filled circles).

magmatism in Hokkaido. The volcanics are HFS element-depleted arc types and show distinct spatial compositional variations between volcanic fields. In both the western (SWH) and eastern (AKS) volcanic fields, across-arc increases in incompatible elements, such as K_2O, can be recognized (Figure 4). Basaltic andesite associations in the back-arc side of the SWH show extremely high enrichments in LIL elements and Zr/Y and Rb/Zr ratios. These spatial variations continue to the main part of the Kuril and northeastern Japan arcs (e.g., Sakuyama and Nesbitt, 1986; Nakagawa et al., 1988; Shibata and Nakamura, 1997). In contrast, the central field (TTS) is characterized by ambiguous across-arc variations and by enrichment in incompatible elements (K_2O, Rb, and Zr) and their ratios (Rb/Sr, Rb/Zr, and Zr/Y), especially in the andesite and dacite. The spatial compositional variations in the volcanics at the arc-arc junction are characterized in terms of the more differentiated nature of the silicic rock from TTS.

Geochemistry and petrography indicate that the compositional variations in each volcano can be best explained by crustal assimi1ation and/or magma mixing between mantle-derived basaltic and crust-derived silicic magmas. Considering that the crustal thicknesses beneath the volcanic fields are almost identical (25-35 km), negative values in the Bouguer anomaly in the TTS (<20 mgal in the TTS vs. 20 mgal < in the other fields) suggest that the crustal materials are less dense, that is, more differentiated (Figure 5). Thus, the more differentiated nature of the TTS andesites and dacites may be derived from their more differentiated underlying crustal materials. The presumed compositional differences in crustal materials beneath Hokkaido are consistent with geological structures formed under varying Cenozoic tectonic settings.

4. Quaternary volcanism in central Hokkaido (TTS volcanic field)

During late Pliocene to early Pleistocene, Tokachi welded tuff, which is composed of more than eight silicic pyroclastic flow deposits, was issued from TTS (Figure 6). These tuffs cover a 1200-km^2 area in central Hokkaido (Ikeda and Mukoyama, 1983). The latest large caldera-forming eruption took place in ca. 1.0 Ma at the Tokachi-Mitsumata caldera located on the northeastern part of TTS (Ishii et al., 2008). After the numerous caldera-forming

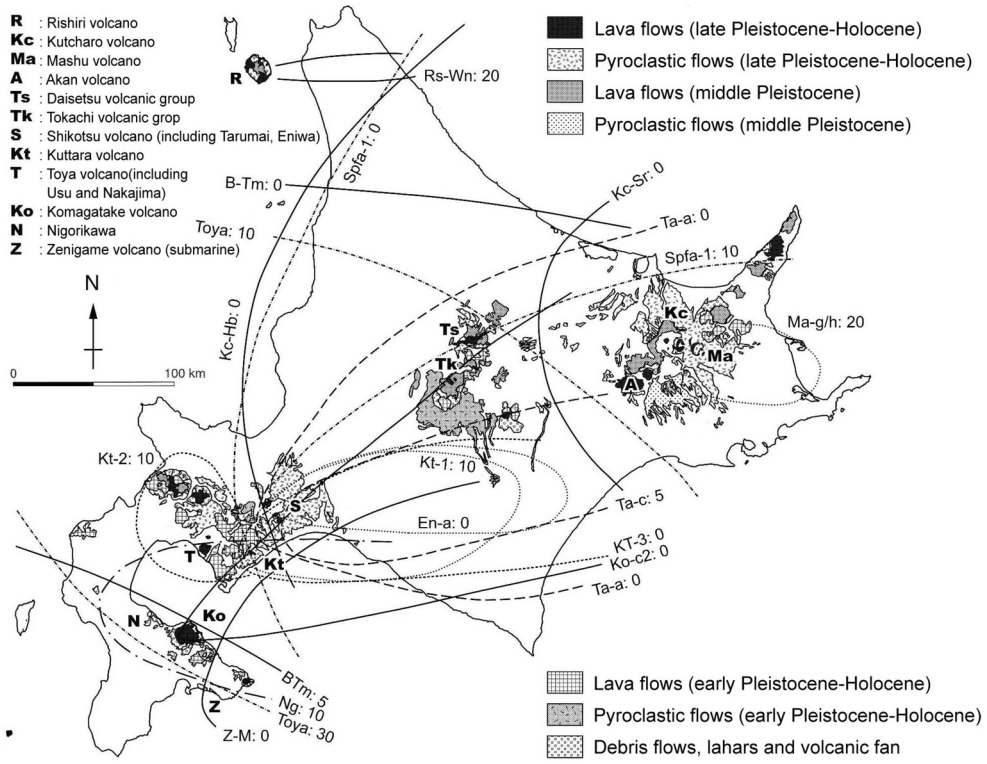

Figure 6. Distribution of Quaternary volcanic rocks in Hokkaido (modified from Okumura, 2003). The isopachs are in cm.

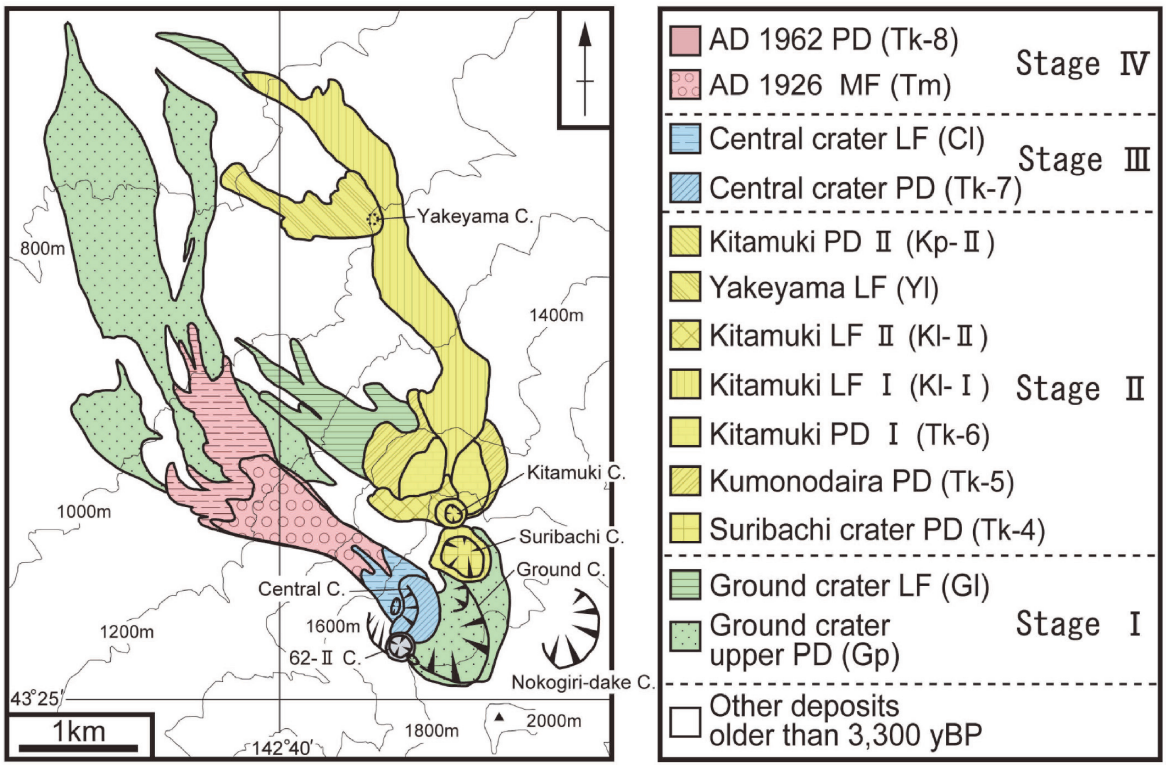

Figure 7. Geological map of Tokachi-dake volcano, showing deposits ejected during the last approximately 3.3 kyr (Fujiwara et al., 2007). The contour lines are at 200-m intervals. PD: pyroclastic deposit, MF: mudflow deposit, LF: lava flow.

eruptions, two volcanic chains began its activity: Nipesotsu-Shikaribetsu and Taisetsu-Tokachi. The Shikaribetsu volcano group is characterized by andesitic dome-forming eruptions that occurred several ten thousands years ago. Although the Nipesotsu volcano group consists of an andesitic stratovolcano and was formed in 0.4 Ma, Maruyama volcano, located at the southern part of Nipesotsu volcano, is one of the active volcanoes in Japan. The Taisetsu (Daisetsu) volcano group locates on the northern part of the Taisetsu-Tokachi volcanic chain and consists of two stratovolcanoes: the Kita (Northern) and Minami (Southern) Taisetsu volcanoes. About ca. 38 ka, the most explosive eruption occurred at the summit area of Taisetsu volcano, producing plinian fall deposits (Ds-Oh) followed by a pyroclastic flow, which formed a small depression, the Ohachidaira caldera (2 km in diameter). Asahi-dake, one of the summit domes of the Taisetsu volcanoes, is still active. The Tokachi volcano group (TVG) is situated on the southwestern end of the Taisetsu-Tokachi volcanic chain. The activity of the TVG has been divided into three groups: Older, Middle, and Younger TVG (Katsui et al., 1963). The structure of the TVG was built up until about 100 ka during the middle stage (NEDO, 1990), forming NE-SW-trending stratovolcanoes and lava domes. Although the early activity of the younger TVG has not yet been clearly revealed, most eruptive activities of this stage occurred at the northwestern flank of the edifice of Tokachi-dake volcano (Figure 7).

4-1. Tokachi-dake volcano

Tokachi-dake volcano, one of the most active volcanoes in Japan, locates at the center of the TVG (Figure 4). Its latest eruptive activity began about 3.3 ka after a long dormancy and has continued at several crater areas until now (Figures 8). Eruptive activity has been recorded only since about 150 years ago. Although phreatic explosions had intermittently occurred during the 19th century, magmatic eruptions occurred in 1926 and 1962. Especially, the 1926 eruption was accompanied by a large mudflow, which killed 144 people. This was the most serious volcanic disaster during that century in Japan. Such a considerable scale of eruptions has not occurred

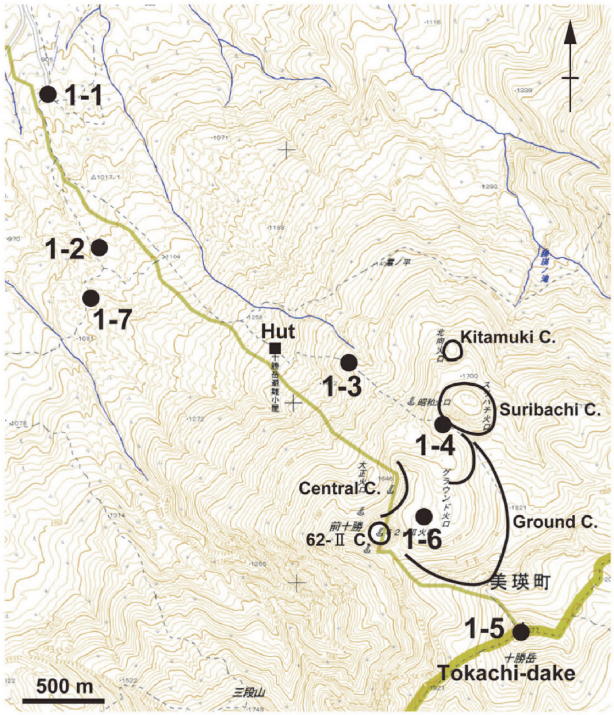

Figure 8. Map showing stops (Day 1) and craters (C.) on the northwestern flank of Tokachi-dake volcano based on parts of topographic maps from Geographical Survey Institute of Japan.

since a moderate magmatic eruption in 1988 - 1989, whereas the level of volcanic activity of Tokachi-dake volcano has remained high until now. This field trip focuses on the activities in the last approximately 3.3 kyr to investigate various types of eruptive deposits.

4-1-1. Eruptive activities during the last 3.3 kyr

On the basis of the locality of source craters and crater areas, the presence of dormancy, and the whole-rock chemistry of juvenile products, the eruptive activities of Tokachi-dake volcano during the last 3.3 kyr can be divided into stages I, II, III, and IV (Fujiwara et al., 2007) (Figure 9).

The eruptive activity of Stage I has been the most explosive and voluminous during the last 3.3 kyr, and generation of pyroclastic flows has been recognized only in this stage (Figure 7). During the eruptive activity, repeated large pyroclastic eruptions had produced pyroclastic flows twice (Ground crater, lower and upper PDs: PD=pyroclastic deposits). The upper one (Gp) occurred in 3.3 ka (Figure 9). The lower one (Tk-2) was associated with pyroclastic falls (Figure 10). These explosive eruptions formed a large crater, named "Ground crater", which can be topographically recognized as a combination of two craters. This is consistent with the repetition of explosive eruptions. These explosive eruptions had been followed by lava effusion, which occurred possibly from the northwestern flank of the Ground crater. After the activity of Stage I, a period of dormancy lasting more than 1 kyr ensued.

In Stage II, the vent positions had moved north of the Ground crater. The explosive eruptions had occurred several times around 1 ka, forming several pyroclastic cones, including Kumonodaira, Suribachi, and Kitamuki I (Figures 9 and 10). After the construction of these cones, lava flows effused from one of the cones. In addition, another lava flow effused from the northwestern foot of Tokachi-dake volcano, forming the Yekeyama crater. The activities of Stage III began with explosive eruptions and formed a pyroclastic cone, the Central cone. Since then, the activity had changed moderately to effuse lava flows repeatedly. The reported ^{14}C age of one of the flows is 280±80 yBP (Ishikawa et al., 1971). According to old reports, no magmatic eruptions occurred during the 19th century.

The eruptive activity progressed to Stage IV in the 20th century, particularly beginning in AD 1926. Although the eruptive volume of ejected magma was not very large, the eruption was accompanied by sector collapse of the Central cone. Immediately following the collapse, a hot (approximately 400 degrees Celsius) hydrothermal surge melted snow and produced a large-scale mudflow that reached more than 25 km in distance, causing significant damage and deaths in the towns downstream (Uesawa, 2008). In AD 1962, a sub-plinian eruption occurred, and scoria falls were distributed on eastern Hokkaido, resulting in the formation of the 62-II cone (Figure 11). Thereafter, vulcanian eruptions from the 62-II cone occurred in 1988-89. During a series of these eruptions, generation of a minor scale of pyroclastic flows and surges was recognized, along with emission of bombs.

In Stages I, II, and III, the eruption style

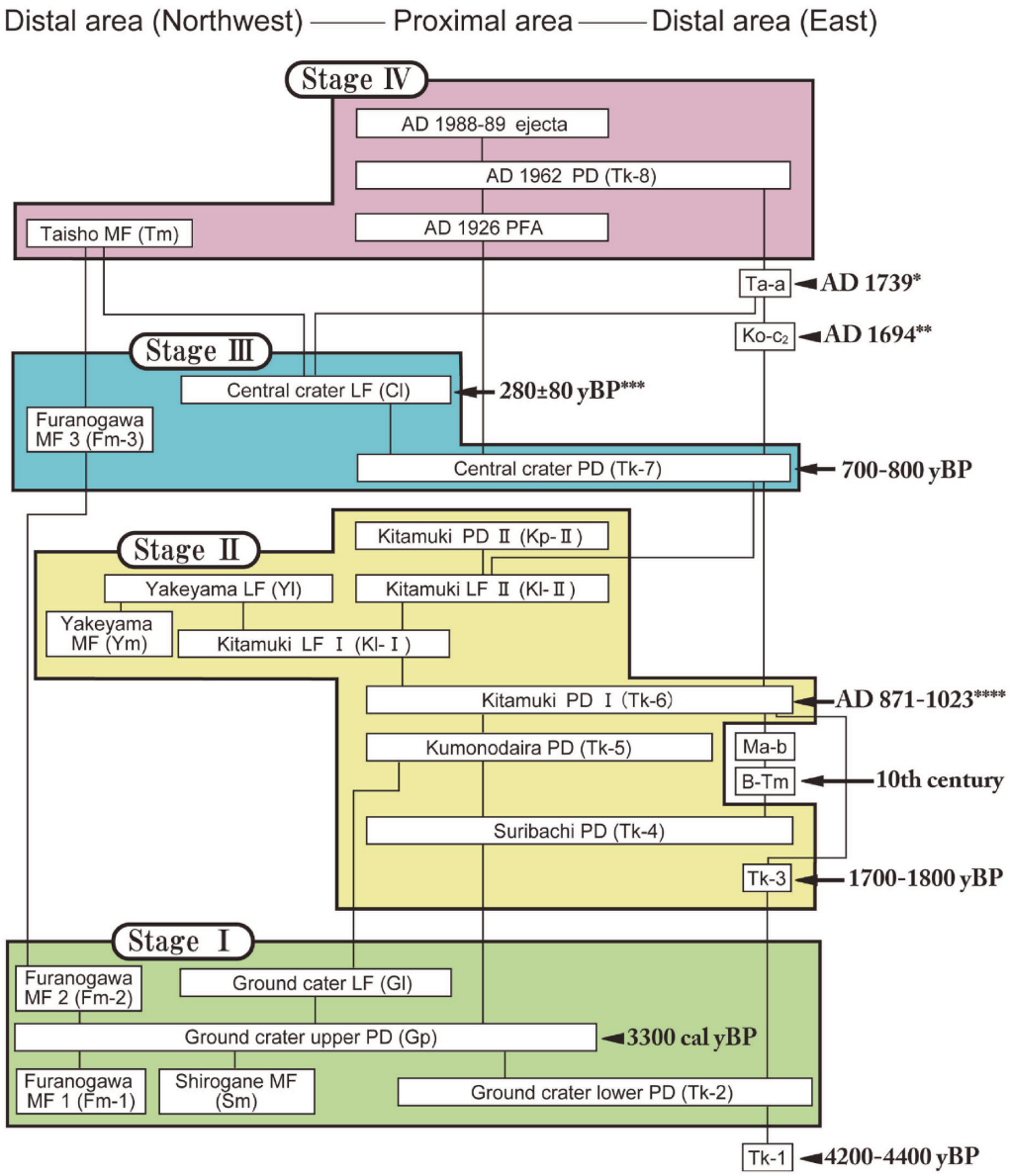

Figure 9. Block diagram showing the volcanic history of Tokachi-dake volcano during the last 4.4 kyr (Fujiwara et al., 2007). Ages: * Katsui and Ishikawa (1981); ** Katsui et al. (1989); *** Ishikawa et al. (1971); **** Ito et al. (1997). PFA: pyroclastic fall deposit, PD: pyroclastic deposits, LF: lava flow, MF: mudflow deposit.

had changed systematically from explosive to effusive eruptions. On the other hand, the eruptive activity of Stage IV has been ongoing. The total volume of eruptive materials during the past 3.3 kyr is estimated to be ca. 0.1 km^3 DRE (Figure 12). The eruptive volume was largest in Stage I (0.040 km^3 DRE) and decreased in the following stages (Stage II, 0.035 km^3 DRE; Stage III, 0.019 km^3 DRE; Stage IV, 0.006 km^3 DRE). The average eruption rate is about 0.03 km^3 DRE/kyr, which seems to be much smaller than the average eruption rate of other active volcanoes in Hokkaido.

4-1-2. Magma system

Although the TVG is composed mainly of andesitic lavas and pyroclasts, the products erupted during the last approximately 3.3 kyr are dominated by mafic rocks (SiO_2=51-60 wt.%). All of the rocks are porphyritic (20-55 vol.% phenocryst content), with phenocrysts of plagioclase, clinopyroxene, orthopyroxene, and magnetite. Olivine microphenocrysts (usually <5 vol.%) are found in basalt to basaltic andesite, whereas minor amounts of ilmenite and quartz phenocrysts are also found in andesitic rocks. The compositional variations of the rocks from Stage I are quite large, whereas

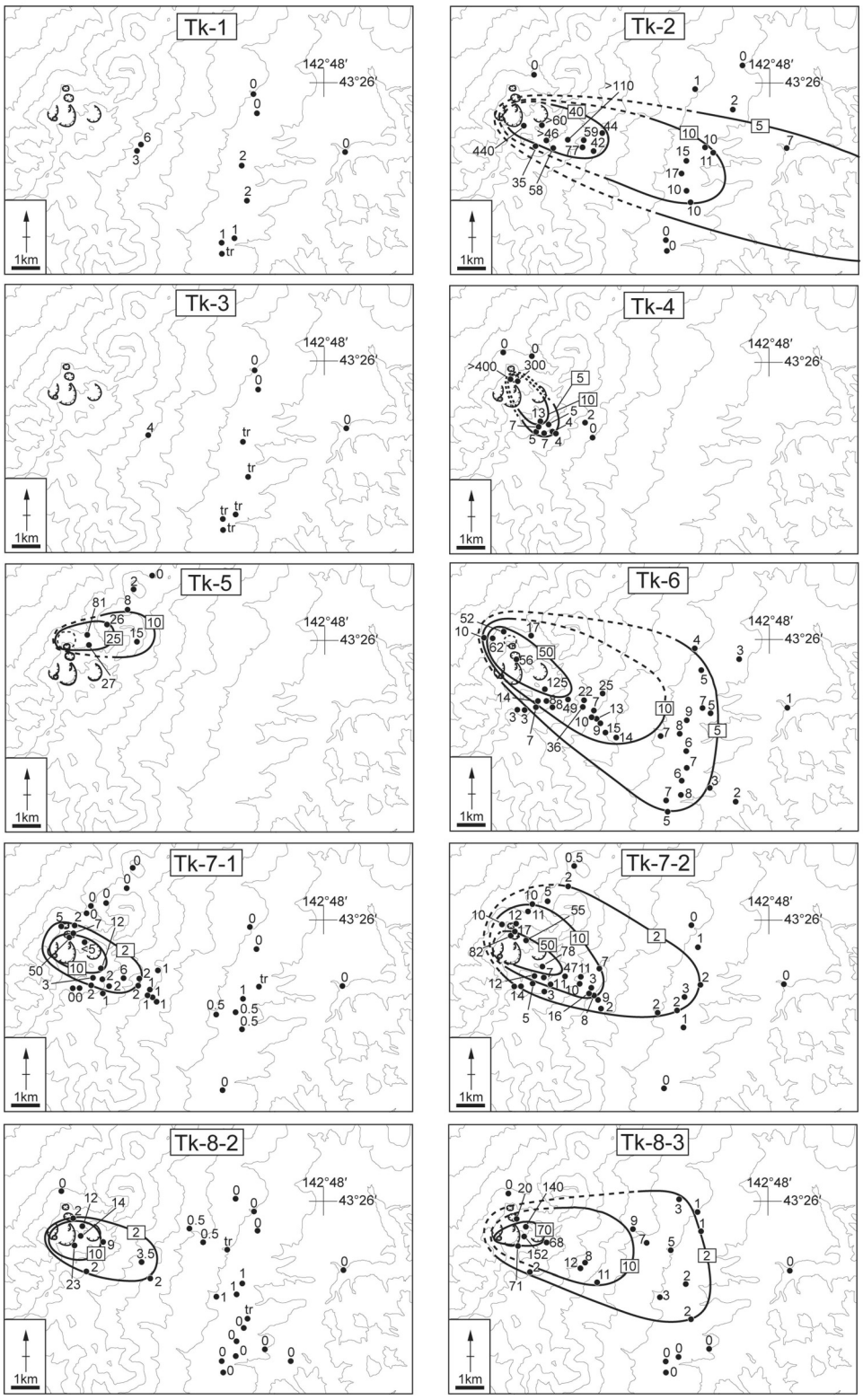

Figure 10. Location and distribution maps of tephra beds from Tokachi-dake volcano to distal areas. Numerals indicate the tephra thickness in centimeters. Contour lines are at 200-m intervals (Fujiwara et al., 2007).

basaltic and basaltic andesitic magmas have been dominant in the subsequent stages (Figure 13). The chemical compositions of the rocks from each stage show distinct features. This helps us to identify the source vent areas of medial and distal eruptive materials (Figure 13).

The rocks from Stage I show various scales of heterogeneity formed by pumice and

Figure 11. Photograph of the 1962 Tokachi-dake eruption (Ishikawa et al., 1971). The eruption cloud reached a maxiheight of 12 km.

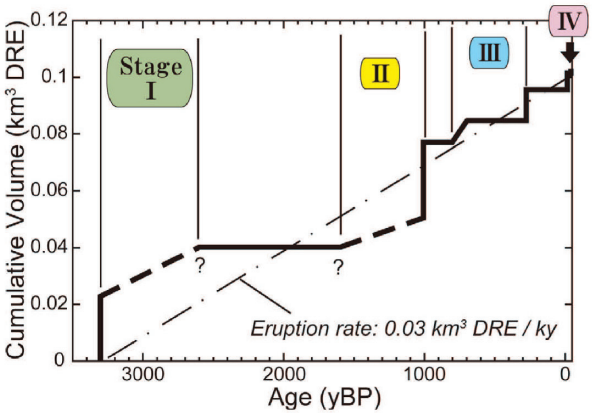

Figure 12. Cumulative magma volume versus time for deposits erupted from Tokachi-dake volcano during the last 3.3 kyr (Fujiwara et al., 2007).

scoria, banded pumice, and heterogeneous groundmass. In addition, the whole-rock chemical compositions of eruptive materials show linear trends on all Harker diagrams, which indicates mixing of two end-member magmas. However, it seems that the mixing process did not progress well because we recognized both heterogeneous features and wide compositional variations in these rocks. Thus, it should be noted that the magma mingling process had occurred during eruptions of Stage I. On the other hand, the heterogeneous features of rocks from the following stages were hardly recognizable. In addition, the compositional variations of these rocks have decreased. However, we recognized the presence of disequilibrium compositional relationships between phenocrystic minerals, olivine, and pyroxenes, for example. This suggests that the magma mixing process has progressed since Stage I.

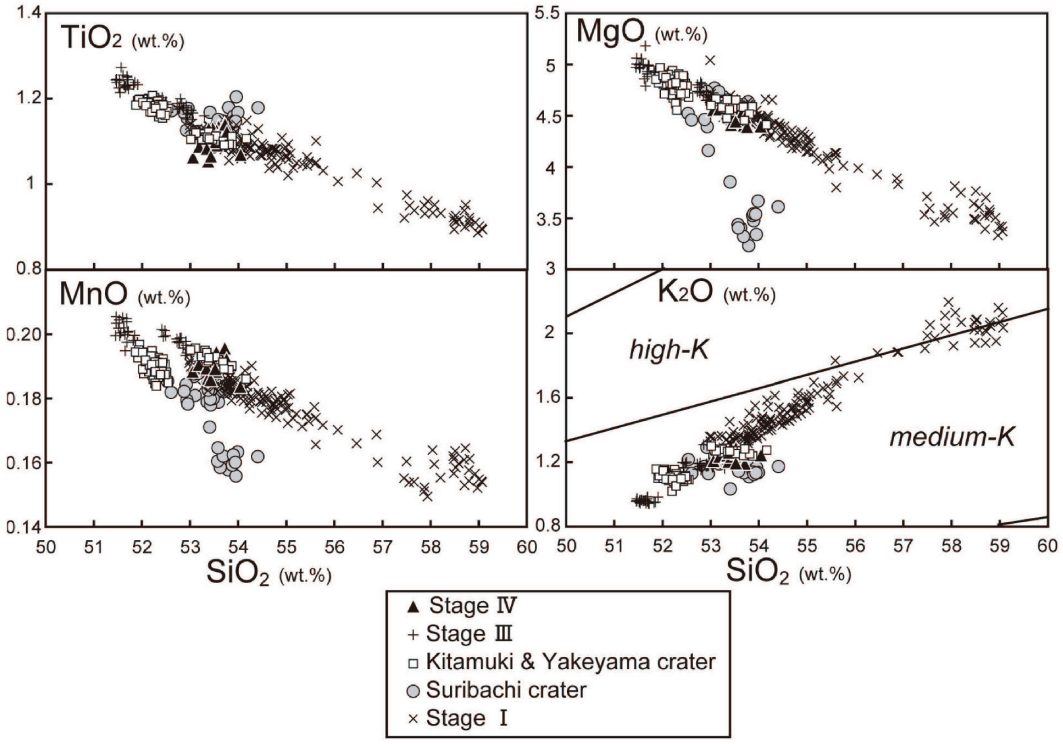

Figure 13. Harker diagrams for Tokachi-dake volcanic rocks erupted during the last approximately 3.3 kyr (modified from Fujiwara et al., 2007). The divisions in the SiO_2 vs. K_2O diagram are from Gill (1981).

5. Quaternary volcanism in Eastern Hokkaido (AKS volcanic field)

The AKS volcanic field consists of the Akan-Shiretoko volcanic chain, extending to the Kuril Islands in the SW-NE direction for 200 km (Figure 1). The volcanic chain composes the echelon alignment with the eastern volcanic islands, such as Kunashiri, Iturpu, and Urup (e.g., Tokuda, 1926), and consists of numerous andesitic stratovolcanoes and three major calderas: Akan, Kutcharo, and Mashu. These calderas are clustered within a 50-km^2 area at the southwestern part of the volcanic chain (Figure 14). The Akan and Kutcharo calderas are more than 20 km in diameter each, whereas Mashu consists of small calderas located on the rim of Kutcharo. In eastern Hokkaido, the concentration of large-scale explosive eruptions (VEI > 5; this high index could be related to caldera formation) has migrated from Akan to Mashu; that is, from west to east (Figure 15) (Hasegawa et al., 2012). More than 70 large-scale explosive eruptions have been recorded from the Akan, Kutcharo, and Mashu caldera volcanoes in the past 1.7 Ma. The total tephra volume of these eruptions is estimated to be approximately 1,000 km^2. The discharge rate increased remarkably from 0.2 km^2/kyr to 2.0 km^2/kyr at approximately 0.2 Ma (Figure 16) and remains high owing to the recent frequent activity of the Mashu caldera. The latest large-scale eruption occurred at approximately 0.9 ka (Kishimoto et al., 2009), resulting in the formation of the 1.5 × 1.2 km Kamuinupuri crater at Mashu (Figure 14). The youngest post-caldera volcanoes, such as Mts. Atosanupuri and Me-Akan, are still active. The Quaternary volcanic rocks in eastern Hokkaido consist of basalt and pyroxene andesite-rhyolite without hydrous minerals. The silicic magmas of the Akan, Kutcharo, and Mashu calderas are clearly distinctive on the K_2O and Ba/Zr versus SiO_2 diagrams (Figure 17).

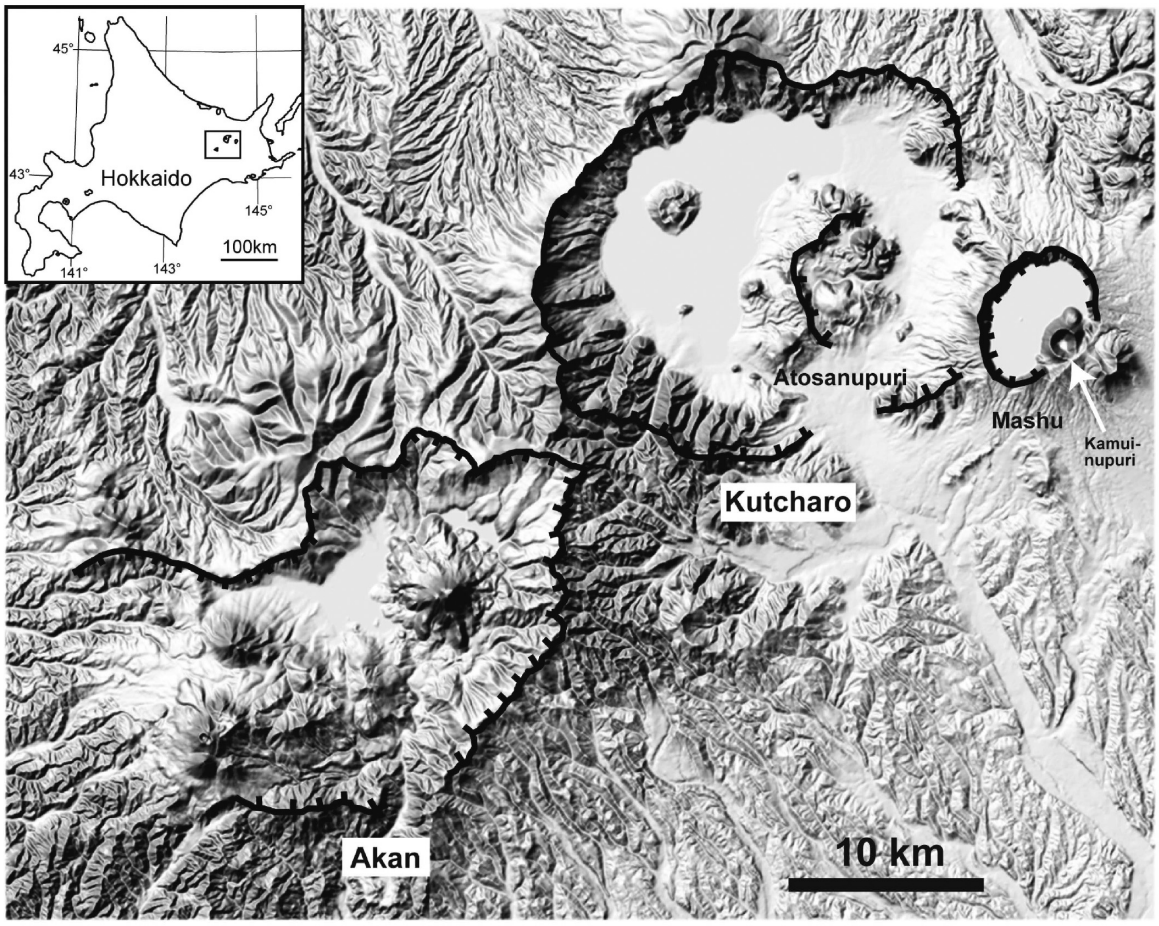

Figure 14. Shaded relief map including the caldera rims, showing the digital topography of the eastern Hokkaido caldera cluster illuminated by light from the northwest direction.

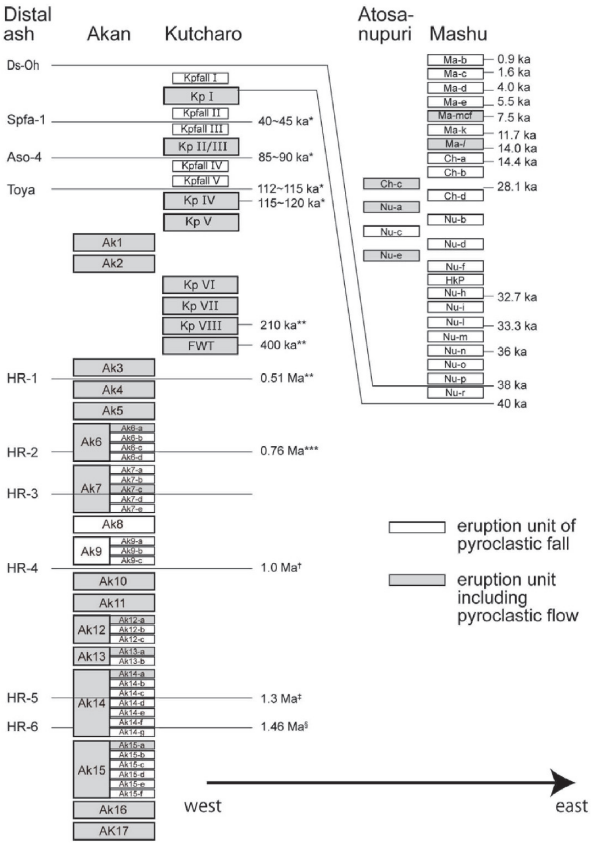

Figure 15. Diagram showing the Quaternary tephrostratigraphy and chronology in eastern Hokkaido. Note that the eruption center has shifted eastward over time. The ^{14}C age data of the Mashu PD were determined by Yamamoto et al. (2010). * Machida and Arai (2003); ** Hasegawa et al., (2011); *** Hasegawa et al. (2008); † Ishii et al. (2008); ‡ Matsui and Matsuzawa (1985); § Sagawa et al. (1984).

5-1. Akan Volcano

Akan volcano is located at the southern end of the Akan-Shiretoko volcanic chain. The volcano consists of a caldera (Akan) and four post-caldera volcanoes (Furebetsu, Fuppushi, O-Akan, and Me-Akan). The Akan caldera is a rectangular-shaped structure (24 km × 13 km) (Figure 18) with a complex history of caldera-forming eruptions. Post-caldera volcanoes are situated inside of the caldera, forming several dammed lakes. Although many post-caldera volcanoes have terminated their activities, Me-Akan volcano has remained highly active. The volcano erupted in 1988, 1996, 1998, 2006, and 2008.

The basement of Akan volcano consists of Cretaceous-Tertiary sedimentary and volcanic rocks, exposed narrowly at the central part of the caldera (Katsui, 1958; Satoh, 1965).

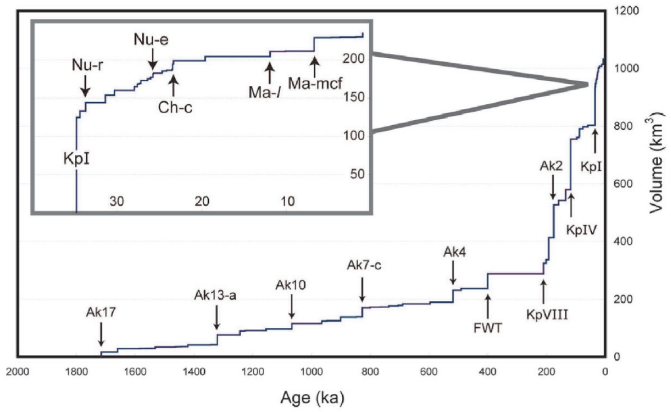

Figure 16. Diagram showing the age vs. the cumulative volume of large-scale eruptions derived from the eastern Hokkaido caldera cluster. It should be noted that the volumes in this figure are not corrected to the dense rock equivalent (DRE).

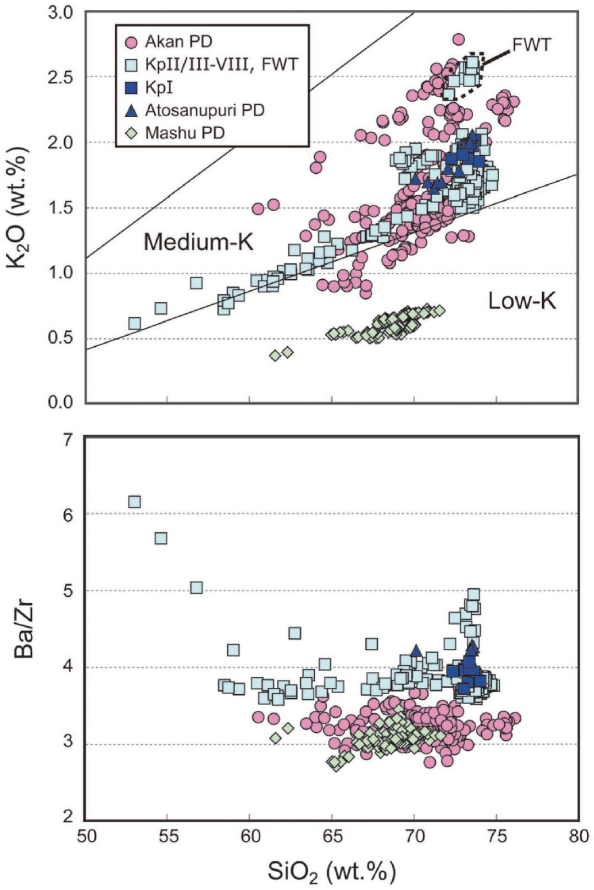

Figure 17. Diagrams of the variations in SiO_2 vs. K_2O (upper) and Ba/Zr (lower) in the whole-rock chemistry of juvenile materials from the Akan, Kutcharo, Atosanupuri, and Mashu PDs. The boundary between low- and medium-K was determined by Gill (1981).

At the rim of the Akan caldera, somma lavas and pyroclastic rocks of basaltic-andesitic compositions are exposed (Figure 18). These are pre-caldera stratovolcanoes, such as Mts. Kikin (995 m) and Iyudaninupuri (902 m). The K-Ar ages of these lavas are 3.9-2.8 Ma (NEDO,

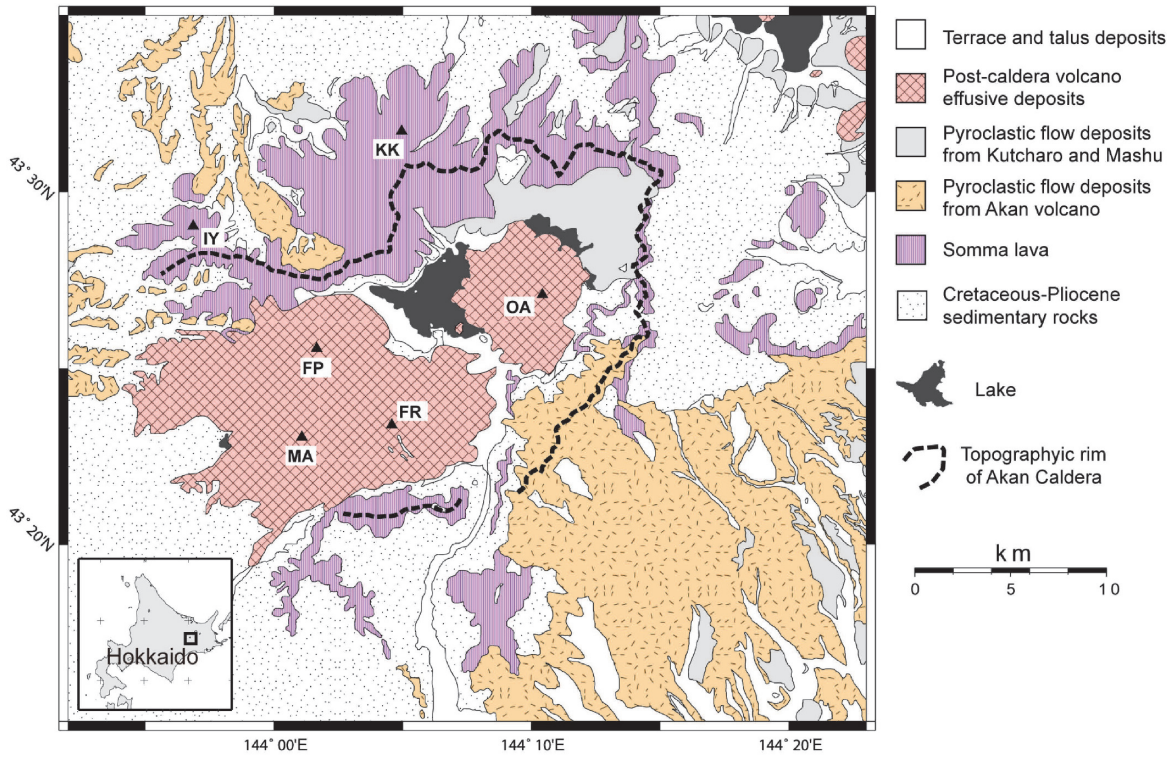

Figure 18. Simplified geologic map around the Akan caldera based on Hasegawa et al. (2006). Closed triangles followed by two letters indicate the major named summits. KK: Mt. Kikin-dake, IY: Mt. Iyudaninupuri, OA: Mt. O-Akan-dake, MA: Mt. Me-Akan-dake, FUP: Mt. Fuppushi-dake, FR: Mt. Furebetsu-dake.

1992; Goto et al., 2000). These ages are much older than those of caldera-forming eruptives, indicating that somma lavas might be independent of caldera-forming magmas.

After a long period of dormancy following the formation of pre-caldera stratovolcanoes, large-scale caldera-forming activities started in the early Pleistocene and continued from 1.7 to 0.2 Ma (Hasegawa and Nakagawa, 2007). Pyroclastic flows and fall deposits related to the formation of the Akan caldera (Akan PD) are distributed in and around the caldera.

5-1-1. Caldera-forming activity
: Stratigraphy

The Akan PD is divided into at least 40 eruptive units, some of which are separated by paleosols that represent significant time intervals between eruptions (Figure 19). These units are classified into 17 eruptive groups, Ak1–Ak17, in descending stratigraphic order, with each group composed of a series of eruptive units (Table 1). Juvenile materials of Ak1-17 are also distinguishable by their petrologic features, such as glass and whole-rock chemistry (Figure 20). Most of the

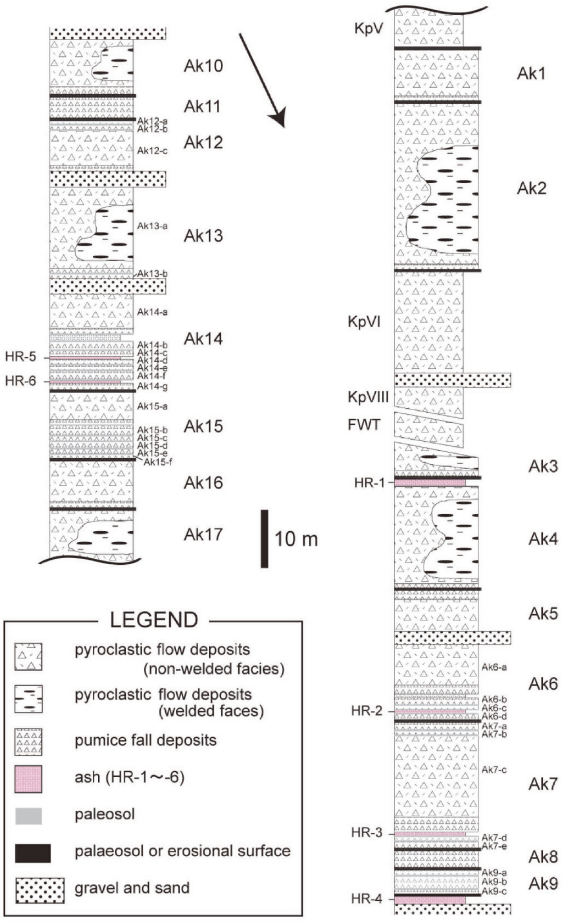

Figure 19. The schematic stratigraphy of Akan pyroclastic deposits.

Table 1. Summary of Ak1-Ak17 and their characteristics. Pfl: pyroclastic flow deposits, Pfa: pumice fall deposits, Wp: white pumice, Gp: gray pumice, Bp: banded pumice, Sc: scoria, Sc/Wp: ratio of Sc to Wp.

	Number of eruptive unit	Facies	Thickness of **Pfl** (average, m)	Degree of welding (**Pfl**)	Types of juveniles	Mineralogy
Ak1	1	**Pfl**+Pfa	30	Non-Middle	Wp	Pl+Opx+Cpx+Opq
Ak2	1	**Pfl**+Pfa	60	Non-Strong	Sc/Wp increase upward	Pl+Opx+Cpx+Pig+Opq
Ak3	1	**Pfl**+Pfa	20	Non-Strong	Sc/Wp increase upward	Pl+Cpx+Opx+Opq+**Ol**
Ak4	1	**Pfl**+Pfa	40	Non-Strong	Sc/Wp increase upward	Pl+Opx+Cpx+Opq
Ak5	1	**Pfl**+Pfa	20	Non	Wp>>Gp=Bp	Pl+Opx+Cpx+Opq
Ak6	4	**Pfl**+Pfa	20	Non	Gp/Wp increase upward	Pl+Opx+Cpx+Opq+**Ol**
Ak7	5	**Pfl**+Pfa	40	Non	Wp>Gp>Bp>>Sc	Pl+Cpx+Opx+Opq+**Ol**
Ak8	1	Pfa	-	-	Gp>>Bp=Sc	Pl+Opx+Cpx+Opq
Ak9	3	Pfa	-	-	Wp>Gp>>Bp=Sc	Pl+Opx+Cpx+Opq
Ak10	1	**Pfl**+Pfa	30	Non-Weak	Sc/Wp increase upward	Pl+Opx+Cpx+Opq
Ak11	1	Pfa	-	-	Wp>Gp>Bp>>Sc	Pl+Opx+Cpx+Opq
Ak12	3	**Pfl**+Pfa	15	Non	Wp>Gp>Bp>>Sc	Pl+Opx+Cpx+Opq
Ak13	2	**Pfl**+Pfa	40	Non-Strong	Sc/Wp increase upward	Pl+Cpx+Opx+Pig+Opq
Ak14	7	**Pfl**+Pfa	15	Non	Gp/Wp increase upward	Pl+Cpx+Opx+Opq+**Ol**
Ak15	6	**Pfl**+Pfa	10	Non	Wp>>Gp>Bp=Sc	Pl+Opx+Cpx+Opq+**Ol**
Ak16	1	**Pfl**+Pfa	30	Non	Wp>>Gp=Bp	Pl+Opx+Cpx+Opq
Ak17	1	**Pfl**	30	Non-Strong	Sc/Wp increase upward	Pl+Opx+Cpx+Opq

groups consist of pumice falls and overlying large-volume pyroclastic flow deposits. Some pyroclastic flows are welded, and the degree of welding increases toward the Akan caldera. The estimated volumes of Ak2, 4, 7, and 13 are particularly large (> 10 km^3 DRE), and Ak2 is the most voluminous (56.8 km^3 DRE) (Table 1).

During the late caldera-forming stage of Akan volcano, another caldera-forming activity started at the adjacent Kutcharo volcano. This is suggested by the relationship of pyroclastic deposits from the Kutcharo caldera interbed between Ak2 and Ak3. Several rhyolitic ash layers (HR1 - HR6, in ascending order) containing hydrous minerals also intercalate in Ak3-Ak17. These exotic layers are correlated with Tokachi welded tuffs derived from central Hokkaido (Hasegawa et al., 2008), suggesting that caldera-forming activities had overlapped in central and eastern Hokkaido during the Quaternary. Such interfingering is helpful in reconstructing the tephro-chronology in this area (Figure 15). The radiometric ages of the exotic tephras range from 1.46 Ma to 0.21 Ma, suggesting that the caldera-forming

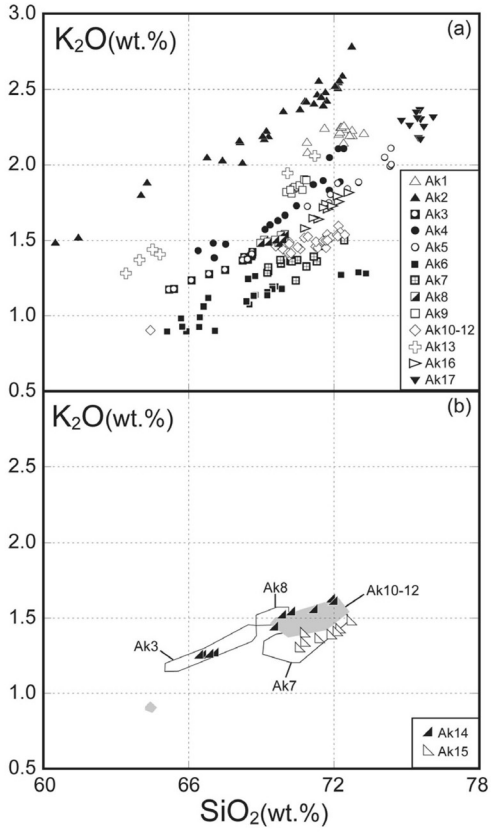

Figure 20. SiO_2-K_2O variation diagrams of the whole-rock chemistry of the Akan PD. (a) All eruptive groups except for Ak14 and Ak15, and (b) Ak14 and Ak15. All data are normalized to 100%.

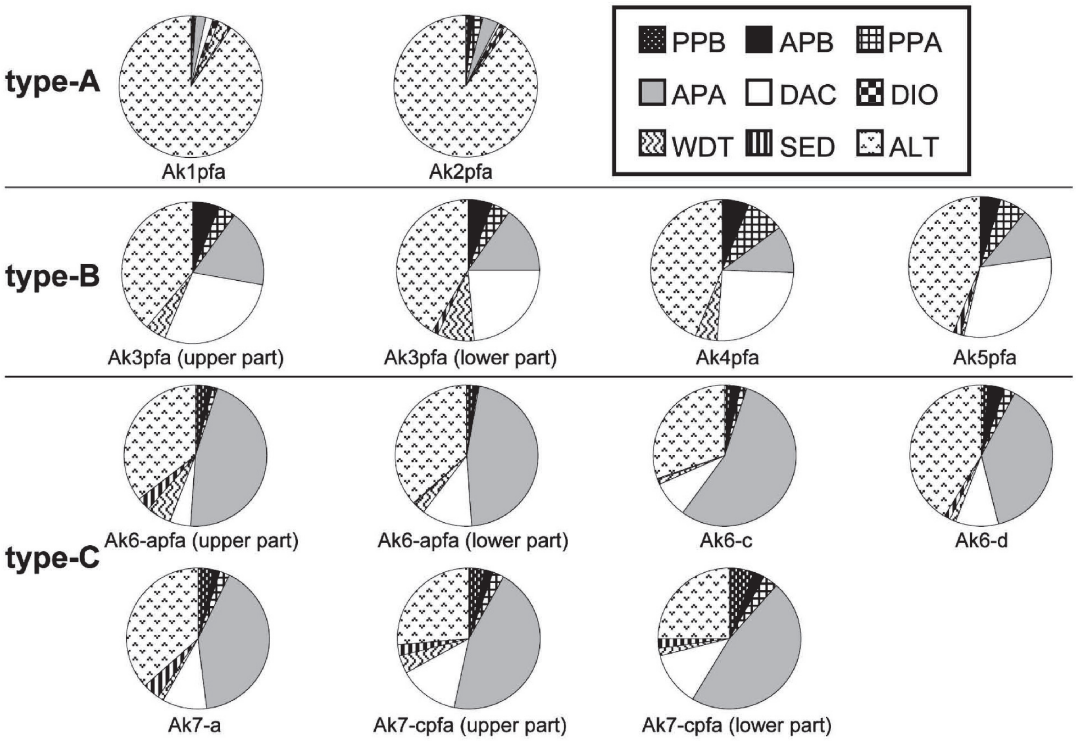

Figure 21. Pie diagrams of rock-type proportions in pumice fall deposits of Ak1 ~ Ak7 (excluding obsidian). PPB: porphyritic basalt, APB: aphyric basalt, PPA: porphyritic andesite, APA: aphyric andesite, DAC: dacite, DIO: diorite, WDT: welded tuff, SED: sedimentary rock, ALT: altered rock.

eruptions of Akan volcano occurred over a period of more than 1 million years.

: Magma system

The juvenile materials of Akan PD are composed of white pumice, gray pumice, banded pumice, and scoria. These are mainly dacite and rhyolite (SiO_2=63.4-76.2 wt.%), with a minor amount of andesite (SiO_2=60.5-62.6 wt.%) (Figure 20). The major phenocrystic minerals in these materials are plagioclase, clinopyroxene, orthopyroxene, and Fe-Ti oxides. Olivine phenocrysts are often contained in Ak3, Ak6-Ak7, and Ak14-Ak15, and pigeonite phenocrysts in Ak2 and Ak13. There is no systematic difference in crystal contents (2-17 wt.%) among the 17 episodes.

The Akan PD is characterized by a wide range of whole-rock K_2O compositions (= 0.8-2.8 wt. %) within a narrow range of SiO_2 compositions (= 67-73 wt. %). On a plot of SiO_2 versus K_2O, each eruptive group forms either a tight cluster or a distinctive linear trend subparallel to one another (Figure 20). This suggests that each eruptive group was derived from a distinct, ephemeral magma system rather than a single long-lived magma system. The temporal changes from one magma system to another can be seen most clearly between Ak6

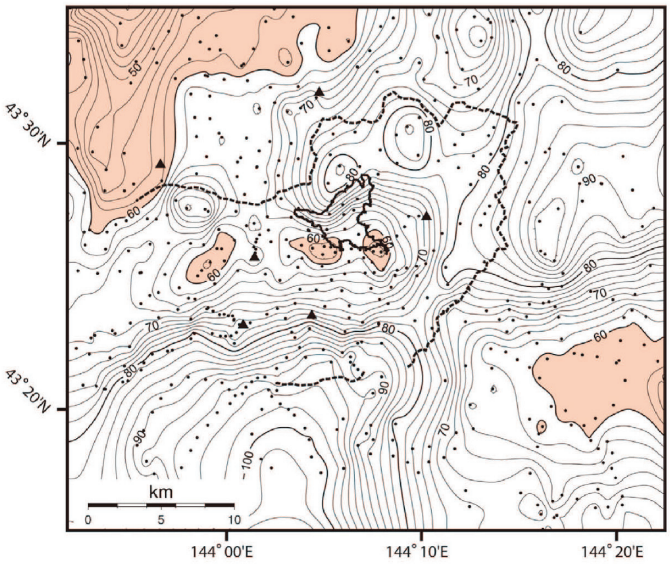

Figure 22. Bouguer anomaly maps of Akan volcano after the lake water correction, with contour intervals of 2 mgal. The reduction density is 2.4 kg m^{-3}. Solid lines indicate the coasts of Lake Akan. Hachured areas show a Bouguer gravity anomaly of less than 60 mgal. Dots and triangles indicate the gravity stations and major summits, respectively.

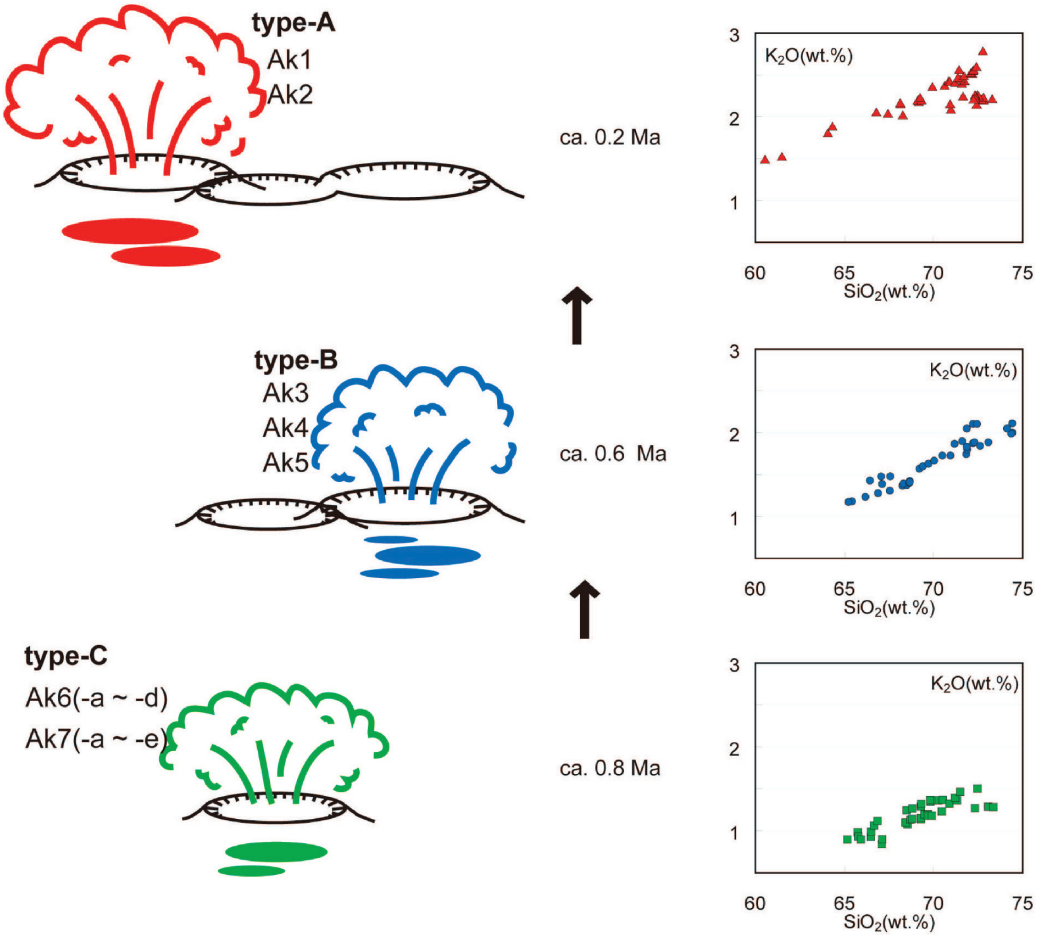

Figure 23. Schematic illustration showing the late evolution of the Akan composite caldera, with a magma composition diagram (SiO_2-K_2O). Multiple magma bodies and their compositional plots are shown; light gray indicates higher K_2O and dark gray denotes lower K_2O contents at a given SiO_2.

and Ak5, and Ak3 and Ak2, where conspicuous stepwise compositional changes occur.

: Model of the caldera-forming process

The present caldera shape is most likely associated with the eruptions of Ak7 to Ak1 (ca. 0.8-0.2 Ma) because these groups are younger and relatively large (>10 km^3DRE each for Ak2, Ak4, and Ak7). These later eruptive groups can be divided into three types based on the lithic components of the pumice fall deposits; the youngest type A (Ak1-Ak2: characterized by altered lithics), the oldest type C (Ak6-Ak7: andesitic lithics), and type B (Ak3-Ak5: dacitic lithics) in between (Figure 21). The temporal changes in the lithic components of the pumice fall deposits suggest that successive plinian eruptions from Akan volcano occurred in at least three distinct vent areas during three discrete periods (Hasegawa et al., 2006).

A Bouguer anomaly map shows that the Akan caldera is characterized by three distinct subcircular closed minima with diameters >4 km, indicating that there are three major depressed segments inside the caldera (Figure 22) (Hasegawa et al., 2009a). These distinct depressions are interpreted as vent areas, which correlate well with the sectorial distribution of the three different lithic types. Vent migration may have occurred at the transitions from Ak6 to Ak5 and from Ak3 to Ak2, where changes in the magma systems are recorded as stepwise compositional changes.

In summary, caldera-forming eruptions of Akan volcano have occurred from at least three distinct vent areas with distinct magma systems over a period of more than 1 million years. As such, the Akan caldera can be described as a composite caldera (in time and space), whose rectangular shape reflects the

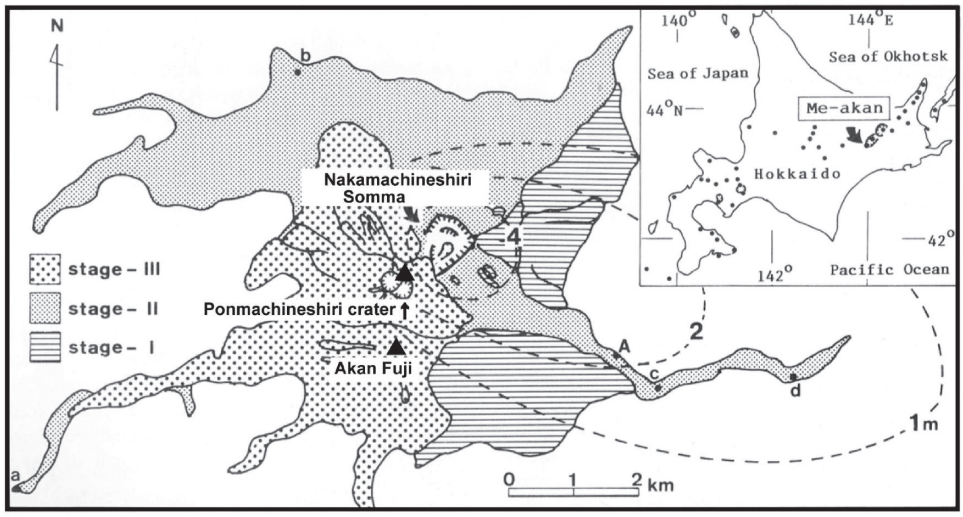

Figure 24. Simplified geologic map of Me-akan volcano (Wada, 1995). Dashed line shows an isopach map of a plinian pumice-scoria fall from Nakamachineshiri somma in Stage II. Solid circles in the inset map indicate Quaternary volcanoes.

distribution of multiple vent areas and related magma bodies (Figure 23).

5-1-2. Post-caldera activity

Among the four post-caldera volcanoes, Frebetsu (1098 m) and Fuppushi (1226 m) are relatively older (0.15 Ma; NEDO, 1992). However, details of their eruptive histories are not revealed because of poor outcrops. These volcanoes consist of one stratovolcano and several lava dome complexes (Yokoyama et al., 1976).

O-akan (1371 m) is an andesitic stratovolcano generated within caldera lakes. It stretches 7 km across at the base and has a height of 950 m (Figure 18). Its first eruption occurred before at least 1.3 ka (Tamada and Nakagawa, 2009). Tens of young lava flows cover the surface of this volcano. The youngest crater at the summit cone is covered by Ma-b, suggesting that the latest magmatic activity occurred before 1 ka. Although the eruption style of O-akan is dominated by effusive lava flows, the volcano had ejected one remarkable tephra layer (Oafa), which is sandwiched between Ma-f (ca. 7.5 ka) and Ta-c (ca. 2.5 ka) (Tamada and Nakagawa, 2009). Based on these data, O-akan was categorized as an active volcano in 2011.

Me-akan volcano (1499 m) is located on the western part of the Akan caldera. This

Figure 25. Aerial photo of the March 2006 eruption of Me-akan volcano (from the northeast direction, by M. Nakagawa). A new crater (on the near side) appeared at the northeastern slope of the Ponmachineshiri crater (on the far side). Blackish ash and mudflow are recognizable on the snowcapped summits. The conical edifice on the right is Akan Fuji.

volcano consists of several volcanic bodies, such as Nakamachineshiri, Ponmachineshiri, and Akan Fuji (Figure 24), and its activity can be divided into three stages (Wada, 1989, 1991). The volcanic activity started at least a few tens of thousands of years ago (Stage I), resulting in older volcanic bodies composed of basaltic andesite to andesitic lavas, which can be observed at the eastern parts of the volcano. The most intensive eruptions occurred in 13,520 ± 240 yBP (Yokoyama et al., 1976), producing the

summit crater of Nakamachineshiri, which is over 1 km in diameter (Stage II). The pyroclastic flow and air fall deposits of this stage contain andesitic scoria and dacitic pumice (Wada, 1995). Another huge explosive eruption occurred ca. 9 ka, also from the Nakamachineshiri crater. In Stage III (ca. 7 ka to present), Ponmachineshiri was generated, forming the highest peak of Me-akan volcano. Akan Fuji is a basaltic-andesitic conical volcano, formed just south of Ponmachineshiri. Two craters of Ponmachineshiri and Nakamachineshiri are still active. In 2006, a small phreatic eruption and related mudflow occurred (Figure 25). The total weight of the 2006 eruption ejecta was estimated to be 9,000 tons (Hirose at al., 2007).

5-2. Kutcharo volcano

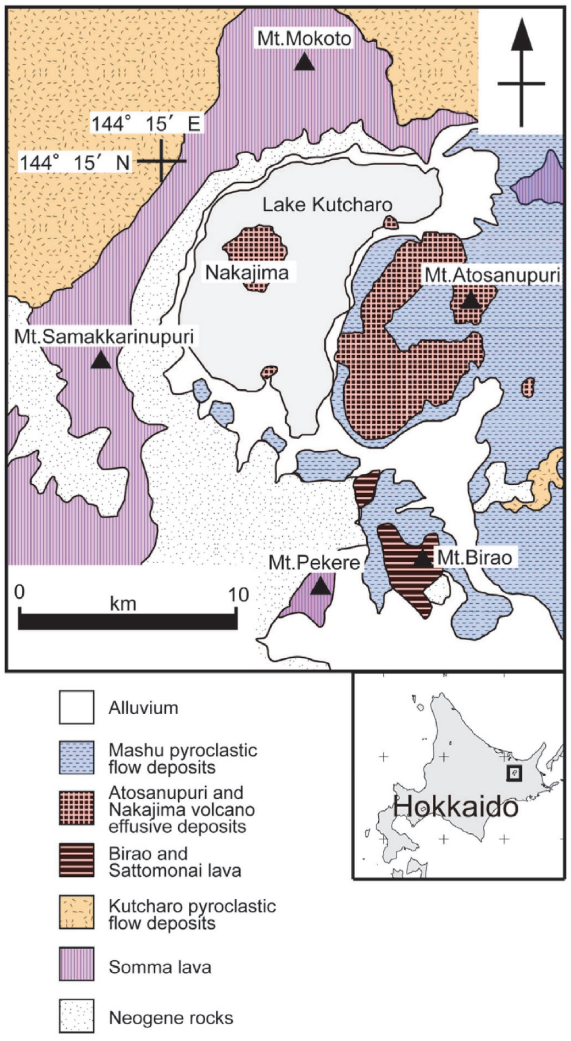

Figure 26. Simplified geologic map of Kutcharo volcano compiled from Hirose and Nakagawa (1995).

Kutcharo volcano consists of a 26 x 20 km caldera (Kutcharo caldera; also called Kussharo), which is the largest in Japan, and three major post-caldera volcanoes (Figure 26): Nakajima, Atosanupuri, and Mashu. Nakajima is a stratovolcano that forms an island in the lake. Atosanupuri consists of a cluster of lava domes and a stratovolcano and fills the eastern half of the caldera. Mashu, a stratovolcano that is younger than the Kutcharo caldera, grew on the east rim of the caldera. The basement of the Kutcharo caldera consists of Miocene-Pliocene sedimentary rocks, which belong to a series of the basement of the Akan-Shiretoko volcanic chain. Before Kutcharo volcano began its activity, early Pleistocene stratovolcanoes of andesitic compositions, i.e., Mts. Mokoto (1000 m), Samakkarinupuri (974 m), and Pekere (732 m), were active around the caldera (Hirose and Nakagawa, 1995) until 0.87 Ma.

5-2-1. Caldera-forming activity : Overview

The caldera-forming eruption began with a large-scale pyroclastic flow that produced Furume welded tuff (FWT) at 400 ka (Figure 15). Subsequent caldera-forming eruption units, the Kutcharo pumice flows VIII–I in ascending order (Kp VIII to Kp I), proceeded during 210 ka–40 ka, with dormancy periods lasting 20 kyr to 40 kyr. Kp III and Kp II are products of the same eruption unit, known

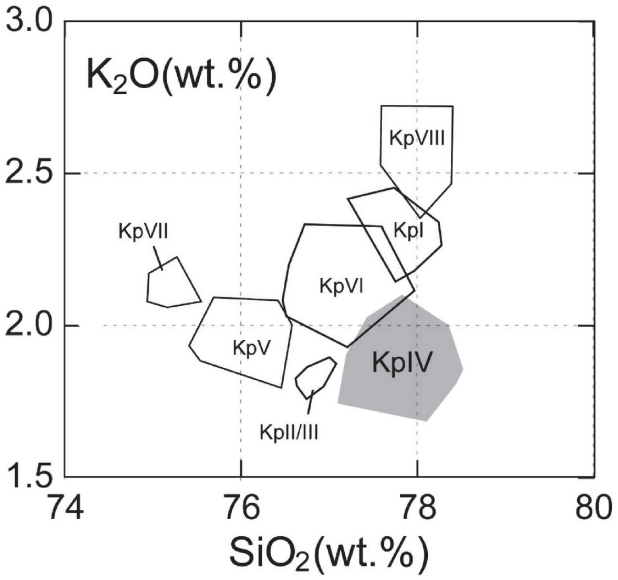

Figure 27. SiO_2-K_2O variation diagram of the glass chemistry of white pumices in the Kutcharo PD. All data are determined by SEM-EDS and normalized to 100%.

as Kp II/III. Kp IV (115 ka–120 ka) is the most voluminous unit at 175 km^3. Five eruption units composed only of pumice falls (Kp V–Kp I) are also recognizable above Kp IV. The total volume of these pyroclastic deposits from the Kutcharo caldera (Kutcharo PD) is estimated to be more than 500 km^3. After the eruption of FWT and Kp IV, Mt. Birao (0.3 Ma) and Sattomonai (95 ka) volcano, respectively, were formed at the southern part of the caldera (Hirose and Nakagawa, 1995). Post-caldera activities could have occurred repeatedly after each large-scale eruption of Kutcharo volcano.

The younger eruptive products, such as Kp II/III and Kp I, abut the inner caldera wall, suggesting that the shape of the present caldera has been mostly defined by the Kp IV eruption (Sumita, 2003). Profiles of the Kutcharo caldera based on boring cores and gravitational surveys show a pan-shaped depressed structure with a ring fracture (e.g., Yahata, 1989; Ichihara et al., 2009). The post-caldera volcanoes (Nakajima and Atosanupuri domes) are arranged along this ring fracture.

Although the juvenile materials of the Kutcharo pyroclastic deposits mainly consist of rhyolitic white pumice, Kp IV contains andesitic scoria and banded pumice. The crystal contents of these materials are relatively large (15-30 wt.%). Although phenocryst minerals of plagioclase, clinopyroxene, orthopyroxene, and Fe-Ti oxides are common in these materials,

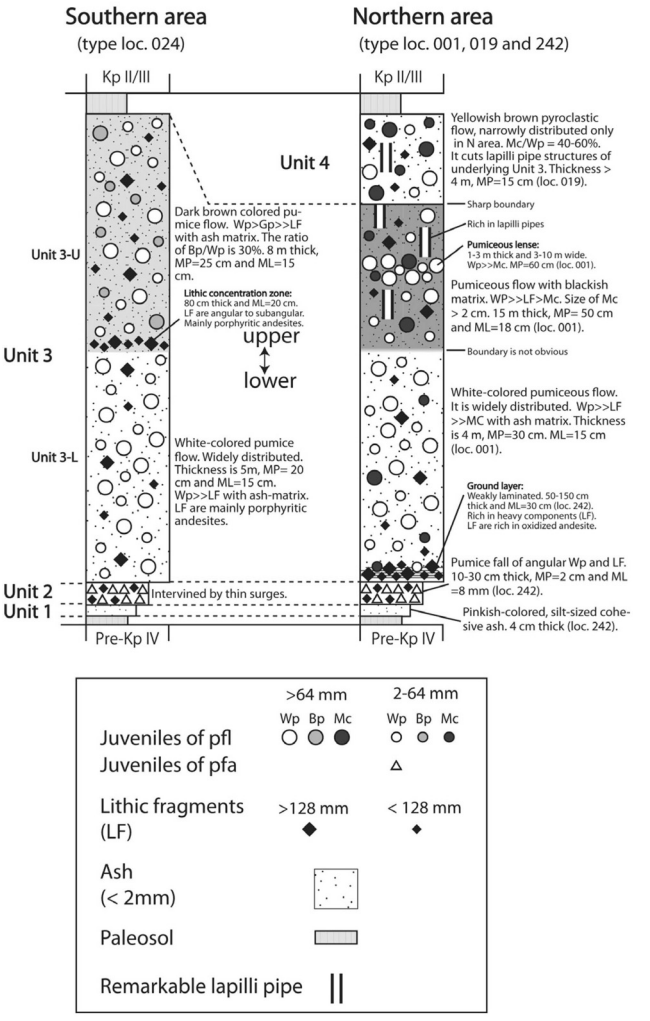

Figure 28. Schematic column of Kp IV at the northern and southern areas, created by combining the columns of the type localities. Wp: white pumice, Bp: brown-tinted pumice, Mc: mafic clasts.

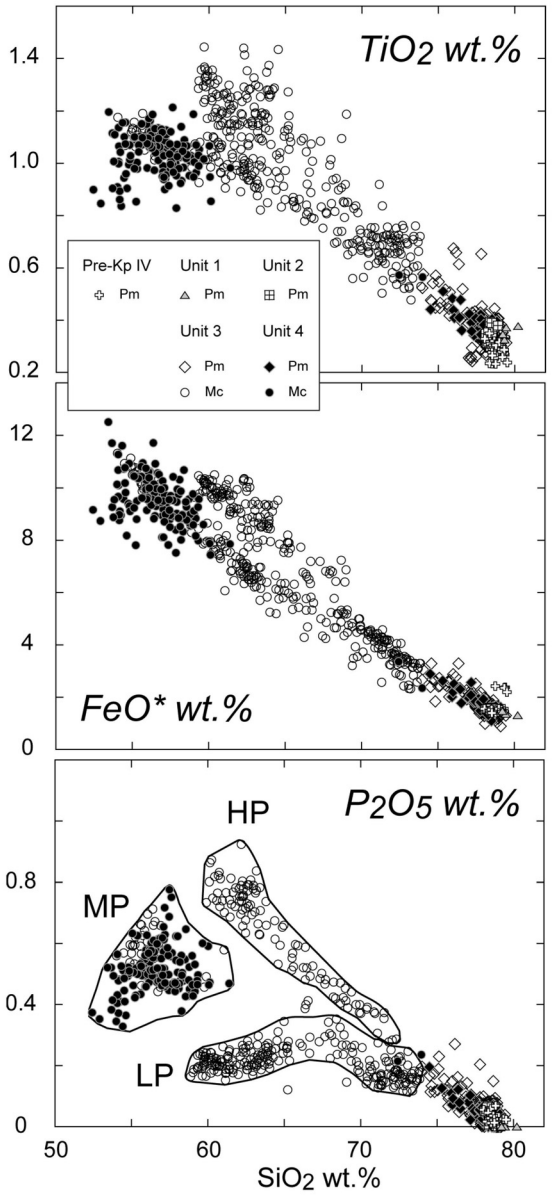

Figure 29. Selected Harker diagrams of the glass compositions of all juvenile materials for Kp IV eruption analyzed by SEM-WDS. Pm: pumice, Mc: mafic clasts.

FWT contains quartz, and Kp I often contains olivine phenocrysts. The Ba/Zr contents of rocks from the Kutcharo pyroclastic deposits are higher than those of rocks from the Akan pyroclastic deposits (Figure 17). The glass chemistry of pumice from the Kuthcaro PD shows different compositional fields between K_2O and SiO_2 diagrams (Figure 27).

: The largest Kp IV eruption

The pyroclastic flow of the largest Kp IV eruption traveled over 50 km in all directions from the source and flowed into the northern Okhotsk and southern Pacific seas. The eruptive age was determined as approximately 120 ka based on the relationship with the overlying widespread tephra from the Toya caldera in southwestern Hokkaido (Figure 15) (Machida and Arai, 2003). The Kp IV eruption deposits can be divided into Units 1 to 4 in ascending order (Figure 28). Unit 1 consists of widely dispersed silt-size cohesive ash. Unit 2 is composed of a thin, poorly sorted pumice fall deposit, characterized by a narrow distribution and small volume (<0.2 km^3). Unit 3 consists of the most voluminous and widely distributed pyroclastic flow deposits. Unit 4 is composed of pyoclastic flow deposits but is distributed over a limited area north of the caldera. The boundary between Units 3 and 4 is usually sharp and sometimes cuts the lapilli pipe structures of Unit 3. This suggests that the final phase (Unit 4) was much smaller than the climactic phase (Unit 3) and that there existed a possible time gap between both units. The juvenile materials of Kp IV mainly consist of pumice (74-78 % in SiO_2) associated with a minor amount of mafic clasts (52-73 % in SiO_2). These mafic clasts are only found in Unit 3 of the northern area and in Unit 4; no mafic clasts exist in Unit 3 of the southern area. According to the SiO_2-P_2O_5 diagram, the mafic clasts can be classified into

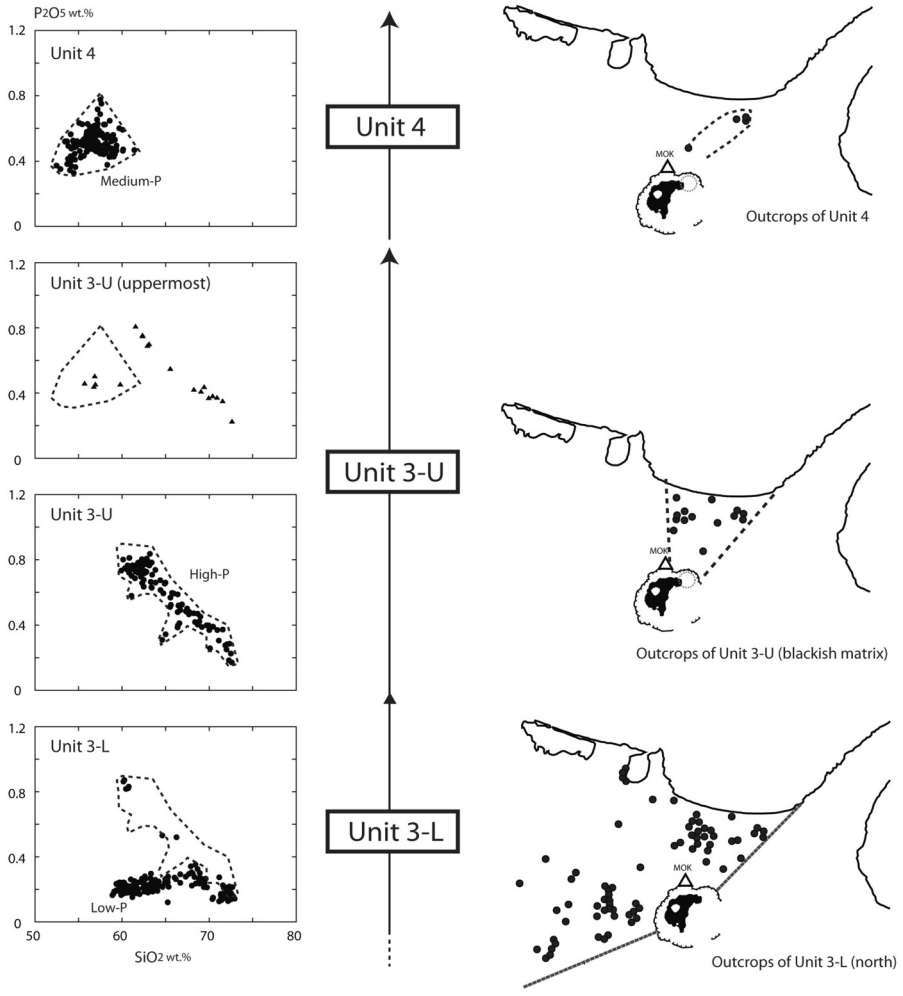

Figure 30. Stratigraphic changes in the matrix glass compositions of mafic clasts in Units 3 and 4 (left), and the plots of outcrops for each unit, including Units 3-L, 3-U, and 4 (right).

three types, which vary in chemistry depending on the stratigraphic level: low P in the lower part of Unit 3, high P in the upper part of Unit 3, and medium P in Unit 4 (Figures 29 and 30). These three types of clasts form three distinct mixing trends in the diagram.

The distinct lithofacies of Unit 3 between the northern and southern areas and the temporal change in the contained mafic clasts, from low-P to high-P types, in the northern

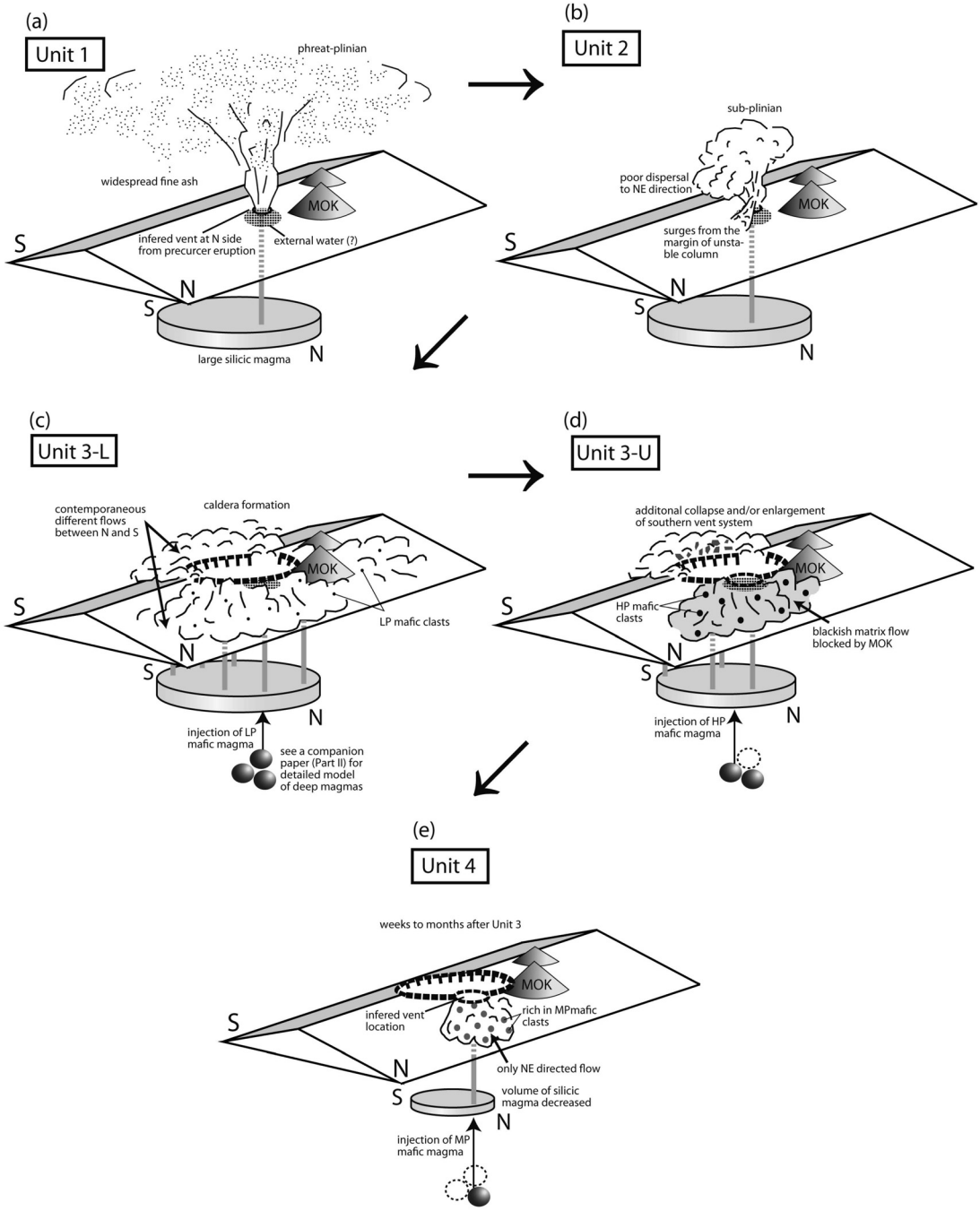

Figure 31. Schematic reconstruction of the Kp IV eruption sequence. (a) Unit 1 (Phase 1) producing widespread fine ash by a phreato-plinian eruption. The vent was possibly located on the northern part of the volcano, where external water (e.g., lake water) was provided from a precursor eruption. (b) A sub-plinian eruption style characterized by a low column height occurred ephemerally in Unit 2 (Phase 2). Pyroclastic surges were intermittently generated from the unstable column. (c) Climactic pyroclastic flows occurred with the caldera formation in Phase 3-1. LP mafic magmas were injected under the northern vent system and produced LP mafic clast-bearing pumiceous flows widely distributed in the northern area (Unit 3-N). Different contemporaneous flows (lacking mafic clasts in the south of Unit 3-L) were generated in the southern area. (d) HP mafic clast-containing flows (Unit 3-N) characterized by a blackish matrix flowed in the northern area. (e) Weeks or months after the deposition of Unit 3, MP mafic clast-bearing Unit 4 flowed narrowly in the northern direction. The volume of silicic magma was considerably decreased in this Unit 4

flows of Unit 3 suggest that the northern and southern flows of Unit 3 could be considered as heterotopic contemporaneous products derived from multiple vent systems (Figure 31-c). This would be consistent with the types of lithic-rich layers in Unit 3. The northern flows of Unit 3 include ground layers that are rich in oxidized andesite. In contrast, the lithic concentration zones of the southern flows of Unit 3 are rich in porphyritic andesite. In the final eruption phase, the northern vent system had been active, erupting medium-P mafic clasts with pumice. These types of magma and their sequence suggest that the three mafic magmas were independently and intermittently injected into the main silicic magma (Figure 31-c~-e). Considering the distribution of deposits containing mafic clasts, it seems that feeder vents for mafic clasts possibly located at the northern area of the caldera erupted voluminous pumice magma, whereas other vents at the southern area only ejected pumice magma. The volume ratio of pumice abruptly decreased in Unit 4, indicating that the silicic magma had been nearly exhausted.

Compared with typical caldera-forming eruptions, the Kp IV eruption lacked a tyical plinian column (Figure 31-b). Thus, it can be concluded that the eruptive activity suddenly reached its climax without forming a stable column. This is possibly due to the development of multiple vent systems in the early stage of the eruption.

5-2-2. Post-caldera activity

After the caldera-forming eruptions, the activity of the young post-caldera volcanoes started ca 40 ka in the Kutcharo caldera. The post-caldera volcanoes consist of Atosanupuri, Nakajima, and Mashu.

Atosanupuri began its activity and grew a stratovolcano before 30 ka. Explosive activities were concentrated around 30 ka, producing Chanai-c (Ch-c) and Nakashumbetsu Upper-a –c and -e (Nu-a, Nu-c, and Nu-e). The largest eruption was Ch-c at 6.9 km^3, after which tens of lava domes mainly of dacitic compositions were generated (Figure 32). The latest eruption took place in 1.3 ka (At-b) and several hundred years ago (At-a) at the

Figure 32. Relief map of Atosanupuri volcano (JMA, 2005).

Atosanupuri dome, which is now a solfatara field.

Nakajima volcano is a pyroclastic cone that consists of base surge and phreatomagmatic deposits. Its eruptions occurred simultaneously with the pyroclastic flows of Atosanupuri volcano (Sumita and Moriya, 2003). Nakajima has a small summit caldera about 1.5 km in diameter, inside of which are effused lava domes.

An activity of Mashu volcano is explained in detail in the next chapter.

5-3. Mashu volcano

Mashu volcano has a caldera (7.5 x 5.5 km in diameter) on the edifice of a stratovolcano, similar to Somma-Vesuvius in Italy. The caldera is famous for its beautiful lake, which has a maximum depth of approximately 210 m. Mashu lake is known as one of the most transparent lakes in the world. On the southeastern rim of the Mashu caldera lies a post-caldera cone of Kamuinupuri (which means mountain of god in Ainu language). Mashu volcano began its activity at 40 ka (Figure 15).

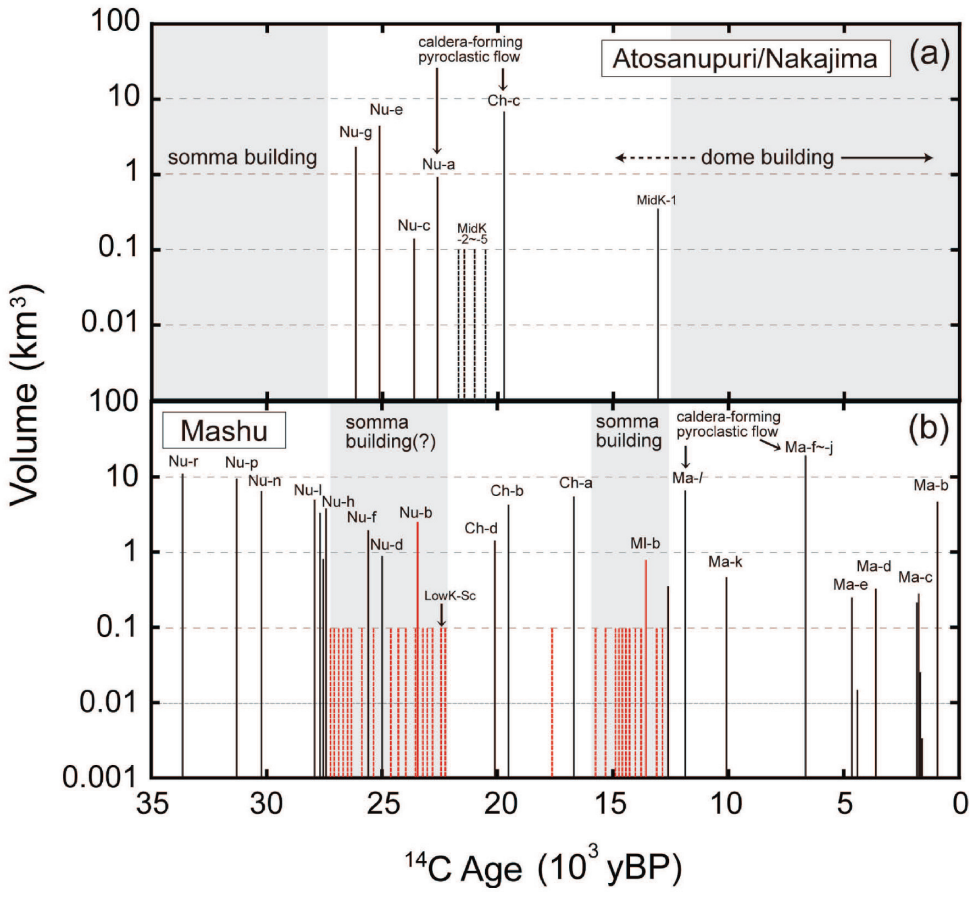

Figure 33. Volumes and ages of explosive eruptions from Atosanupuri/Nakajima volcanoes (a) and Mashu volcano (b). Gray (red in color version) bars denote scoria-dominant eruptions. The volumes denoted by dashed bars (0.1 km^3) are minimum estimations.

The present Mashu caldera and Kamuinupuri crater were formed by large-scale explosive eruptions after 14 ka. These deposits are denoted as Ma-b (0.9 ka) to Ma-l (14 ka) in descending order. The largest eruption unit at 18.6 km^3, known as the Mashu main caldera-forming eruption (Ma-mcf), consists of deposits Ma-j–Ma-f, the age of which was estimated to be 7.5 ka. The 4.6 km^3 Ma-b eruption resulted in the formation of the Kamuinupuri crater. Ma-l is also a large eruption unit at 6.6 km^3. Between Ma-l and Kp I (the youngest caldera-forming eruption of the Kutcharo caldera: 40 ka), at least 15 large-scale eruption units are described, including Nu-r, Nu-p, Nu-o, Nu-n–Nu-l, Nu-i, Nu-h, Higashikayano Pumice (HkP), Nu-f, Nu-d, Nu-b, Ch-d, Ch-b, and Ch-a (Figure 15). Widespread 38-ka Daisetsu Ohachidaira (Ds-Oh) tephra from central Hokkaido is sandwiched between Nu-r and Nu-p (Hasegawa et al., 2009b). Overall, Mashu volcano produced more than 50 plinian eruptions (Mashu PD: total tephra volume >90 km^3) over the period from 40 ka to present, with no dormant periods exceeding several thousand years. On the other hand, only 10 explosive eruptions (total tephra volume = 16 km^3)

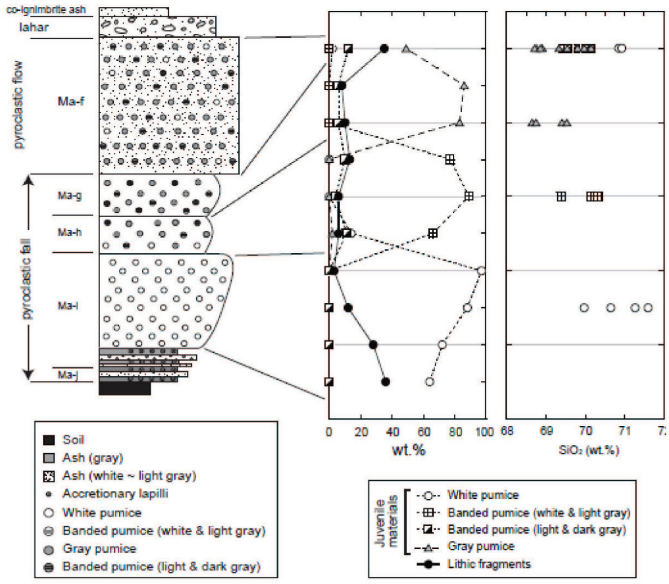

Figure 34. Stratigraphic variations of the rock-type proportions (left) and whole-rock SiO2 content of juvenile materials (right) during the Mashu caldera-forming eruption.

occurred at the Atosanupuri and Nakajima volcanoes over the limited period of 30 to 15 ka (Figure 33).

The juvenile materials of the Mashu PD are commonly aphyric (1~6 %) two-pyroxene andesite to dacite. These characteristically have an extremely low K_2O content and can be clearly distinguished from the products of the adjacent Akan and Kutcharo calderas (Figure 17).

5-3-1. Mashu main caldera-forming eruption (Ma-mcf)

: Stratigraphy

The eruption deposit of Ma-mcf is composed of (1) preceding plinian falls, (2) a climactic pyroclastic flows and (3) co-ignimbrite ash deposits. Within these, there are no soil layers that indicate significant dormancy of eruption. The plinian falls can be further subdivided into four units (Ma-j to Ma-g in ascending order) based on their grain size and the ratio of types of pyroclastic materials (Figure 34). The pyroclastic flow (denoted as Ma-f) that followed was thick and voluminous (the eruption volume was approximately 10 km^3), traveled over 30 km, and was deposited in the adjacent Akan caldera. The co-ignimbrite ash formed a widely distributed layer with an average thickness of about 10 cm.

In addition, lahar deposits were recognized between Ma-f and co-ignimbrite. The lahar deposit is poorly sorted and contains a lot of round and angular grayish pumice clasts and lithic fragments. The types of juvenile materials in the Ma-mcf deposits are characteristically varied, consisting of white pumice, gray pumice, and banded pumice that show streaks of white and light-gray or dark and light-gray pumice.

: Eruption process

The sequence of the main caldera-forming eruption of Mashu will be reconstructed on the basis of a facies analysis and the temporal changes in the lithic/juvenile ratio of pyroclastic deposits during the eruption (Figure 34). The hazardous caldera-forming event of Mashu volcano was initiated by a relatively small explosive eruption from Ma-j. This unit is dominant in lithic fragments, which is indicative of a vent-opening event. Small amounts of the juvenile materials consisted of fine sand-sized, poorly vesiculated blocky ash with accretionary lapilli, suggesting that the phreatomagmatic eruption style was caused by the interaction of water and magma (e.g., Wohletz, 1983).

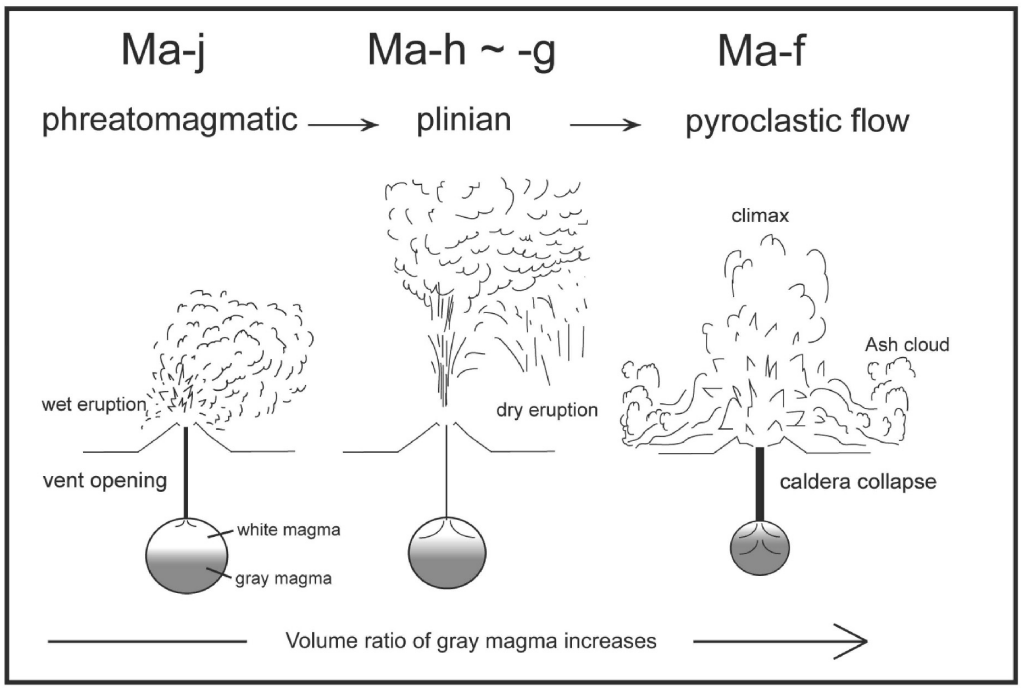

Figure 35. Schematic illustrations of the eruptive sequence of magma systems during the Mashu caldera-forming eruption.

The next unit, Ma-i, is relatively thick and has fewer lithic fragments. The ratio of juvenile/lithic fragments increased with time and reached nearly 100% at the top of this unit, which suggests that the vent system was becoming more stable and that conditions were moving from wet to dry. The eruption style of Ma-i is typically described as plinian. The eruption column height and wind speed at that time are estimated to be more than 30 km and 70 m/s, respectively, according to the methods of Carey and Sparks (1986) for analyzing clast dispersal data. In Ma-h and -g, the plinian eruption style demonstrated that a lower lithic/juvenile ratio had continued and that the catastrophic pyroclastic flow (Ma-f) had finally occurred. The pyroclastic flow discharged voluminous magmas and a lot of lithic fragments because of the caldera collapse.

The Ma-f traveled over the 570-m-high wall of the Akan caldera and was deposited in the caldera basin. The maximum velocity of the ignimbrite was calculated to be more than 100 m/s, as determined by the law of conservation of energy ($v = \sqrt{2gh}$; g=9.8 m/s2, h=570 m). This value is higher than that of any other directly observed pyroclastic flow in the world. A hazardous lahar event accompanied the Ma-f. The composition of the gray pumice clasts in the lahar deposits are the same as that of the juvenile pumice in the Ma-f, which suggests that the lahar had eroded and the pyroclastic debris of Ma-f had been introduced. Either during or after the deposition of the lahar, the co-ignimbrite ash cloud began to settle across the broad area of eastern Hokkaido.

: Magma System

The existence of banded pumice and a linear chemical trend of juvenile materials in the Harker diagram (Figure 17) indicate that magma integration of the two end-members was the main magmatic process during the caldera-forming eruption. The SiO_2 content is highest (70~72%) in the white pumice and lowest (68-70%) in the gray pumice (Figure 34). On the other hand, the banded pumice shows intermediate compositions of SiO_2 (69-71%). During the Ma-mcf eruption, white pumice was abundant in the early units (such as Ma-j and -i), whereas gray pumice increased in the later units (Ma-g to Ma-f). Banded pumice is easily recognizable in the middle unit (Ma-h). These temporal changes in the types of juvenile materials suggest that there was a zoned magma chamber composed of more silicic magma (providing white pumice) and less silicic magma (providing gray pumice) just before the caldera-forming eruption (Figure 35). The steep decline in the ratio of white pumice in Ma-h indicates that most of the upper silicic magma had been ejected during the early units. In the middle unit, the two end-member magmas (white and gray) mingled and were ejected as banded pumice. Finally, the climactic pyroclastic flow primarily discharged gray pumice from the remaining less silicic magma system.

DESCRIPTION OF FIELD TRIP STOPS

Day 1
Tokachi-dake trekking

STOP 1-1: Overview of the Tokachi-dake volcano group (Bogakudai)

This spot is about 930 m a.s.l. on the northwestern foot of Tokachi-dake volcano. The 62-II crater (formed in the AD 1962 eruption: Figure 8) emits abundant steam. The neighboring Central crater, part of which collapsed in the AD 1926 eruption, also emits some steam. The tongue-shaped lava flows of the last 3.3 kyr are clearly visible. Mountain tracks are laid on gravel originated from the AD 1926 mudflows.

STOP 1-2. Pyroclastic flows from the Ground crater

The pyroclastic flow deposits from the Ground crater are exposed on this outcrop (Figures 7 and 9). The upper flow deposits (Gp) are divided into two units based on their matrix color. The lower unit of Gfl-1 has a brownish matrix including abundant lithic fragments, as well as scoria, pumice, and banded pumice as juvenile materials (Figure 36). The abundance of lithic fragments in the deposit indicates that sector collapse might have been generated at the

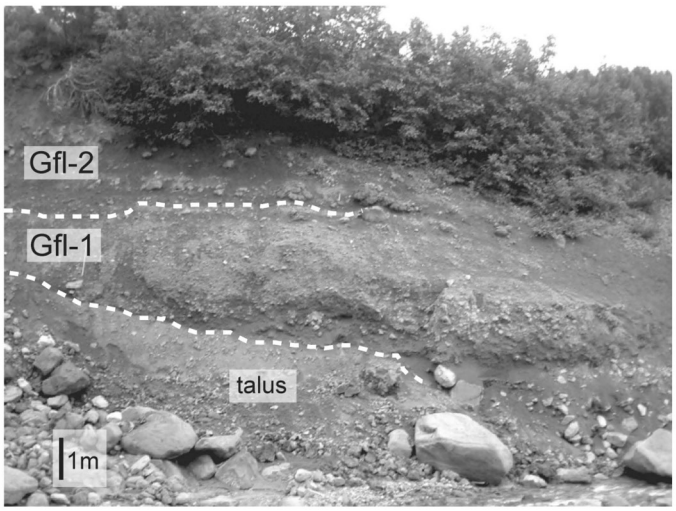

Figure 36. Outcrop photograph of Ground crater pyroclastic flow deposits (Fujiwara et al., 2007). Gfl-2 is directly covered by Gfl-1.

same time. Nevertheless, charcoaled woods suggest a considerably high temperature during their emplacement. On the other hand, the upper unit of Gfl-2 consists of a black matrix including scoria and less abundant lithic fragments. There is no evidence for a dormancy period between the two units. Below the pyroclastic flows, some white-to-gray mudflow deposits and thin soils can be recognized. Moreover, near the bottom of this outcrop, a brown or reddish-brown layer can be seen. This layer is a newly found pyroclastic flow, Gfl-0, the ^{14}C age of which was determined as 3440±40 yBP based on charcoal from the soil just above the flow (Fujiwara et al., 2009).

STOP 1-3. Kitamuki lava flow II

The basaltic lava flows of Stage II effused toward the north and the west from Kitamuki crater (Figure 37). These are called Kitamuki lava flow I and II, respectively. Kitamuki lava flow II is composed of at least three flow units and has a maximum thickness of more than 20 m. At this spot, we can see the topographic features of the lava flow.

STOP 1-4. Suribachi crater

The Suribachi crater is a nearly circular crater about 300 m in diameter (Figure 8). At least four agglutinates are exposed on the southern-to-eastern wall of the crater. Each of these deposits can be distinguished by their

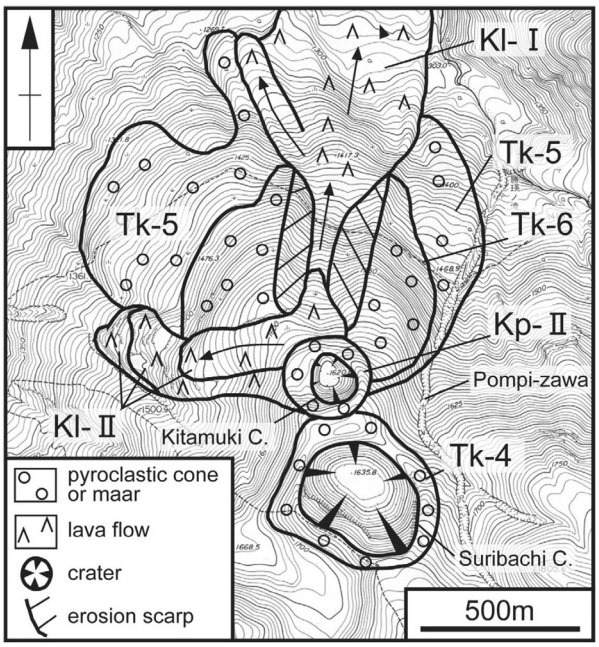

Figure 37. Geological map (Fujiwara et al., 2007) showing pyroclastic cones and lava flows of Stage II drawn on the basemap published by the Geographical Survey Institute. Arrows show directions of lava flow. Abbreviations are same as those in Figure 9.

chemical compositions. The uppermost unit was dispersed toward eastern area, whereas the other units could not be recognized except on the crater wall.

These agglutinates are covered by scoria falls erupted from the Kitamuki, Central, and 62-II craters, suggesting that the activity of this crater ended at least 1 ka.

STOP 1-5. Summit of Tokachi-dake

The summit of Tokachi-dake volcano (2077 m a.s.l.) consists of an andesitic lava dome (60.7 wt.% SiO_2, based on Katsui et al., 1963) estimated to have formed at about 0.1 Ma, according to K-Ar dating (NEDO, 1990). If the weather permits, we may see the entire Taisetsu-Tokachi volcanic chain, the Nipesotsu volcanic groups, the Hidaka chain, and so on.

STOP 1-6. AD 1988-89 volcanic bomb

In AD 1988-89, volcanic bombs were ejected to the north and the northeast from the 62-II crater. These bombs were associated with very small-scale pyroclastic flows (about 5×104 m^3, based on Katsui et al., 1990). Several bombs can be found in the Ground crater,

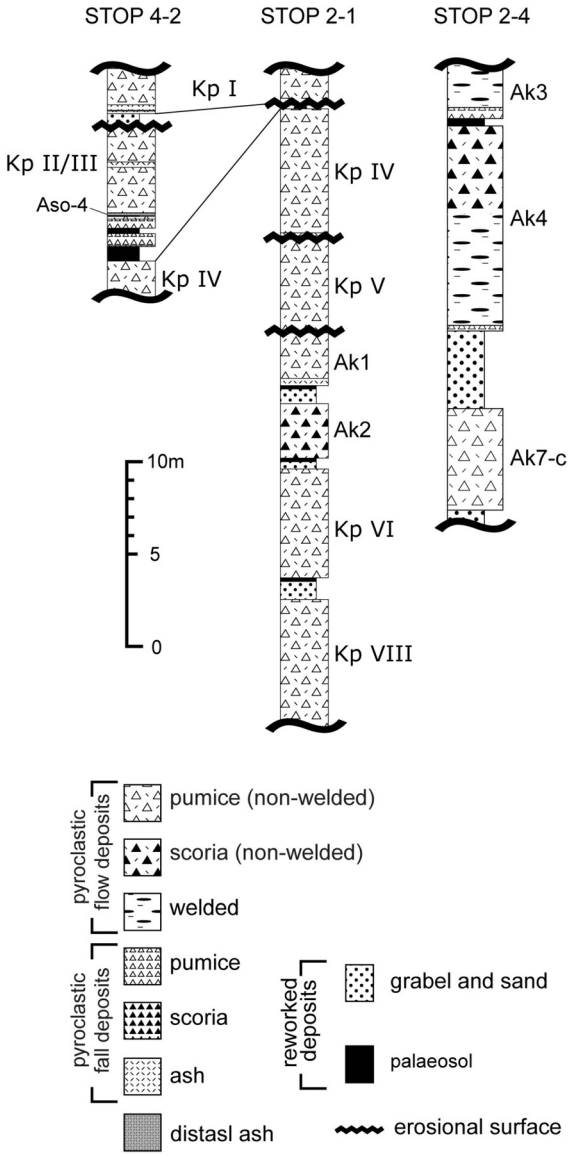

Figure 38. Geological columns of STOP 2-1, 2-4 and 4-2.

ranging from tens of centimeters to 20 meters in length. Some are depressed, indicating that they did not completely solidify on landing. Impact craters formed by hitting the ground can also be seen.

STOP 1-7. Central crater lava flow

The Central crater lava flow (Cl) positioned on the northwestern foot of the volcano consists of some flow units, the ^{14}C age of which was determined as 280±80 yBP (Ishikawa et al., 1971). The topographic features of the lava flow can be observed.

Day 2
Akan caldera-forming eruptions

STOP 2-1: Interfingering of caldera-forming eruption between Akan and Kutcharo volcanoes (Kaisei)

Seven pyroclastic flow deposits can be observed here, including Kp VIII, Kp VI, Ak2, Ak1, Kp V, Kp IV, and Kp I in ascending order (Figure 38). Pyroclastic flow deposits of Ak2 and Ak1 can be recognized between those of Kp VI and Kp V (Figure 15). Although seven pyroclastic flows show the same mineral assemblage (Pl + Opx + Cpx + Opq), the Akan and Kutcharo pyroclastic deposits are distinguishable by their whole-rock chemistry (Figure 17).

STOP 2-2: Proximal facies of the second youngest Akan pyroclastic deposit Ak2 (Senpoku pass)

Proximal facies of the Ak2 pyroclastic deposit can be observed beside the northern rim of the Akan caldera. The deposit consists of clast-supported blocky scoria, pumice, juvenile obsidian clasts, and some accessory lithic fragments. The diameters of the clasts range from 1 to 50 cm. The lower part of the deposit is relatively lithic and pumice-rich, whereas the upper part contains more scoria.

STOP 2-3: Interfingering of caldera-forming eruption between central and eastern Hokkaido (Teshibetsu)

A sequence of Ak5, Ak6, and Ak7 can be observed in this spot. An exotic ash layer, which characteristically includes biotite, is interbedded within Ak7 (Figures 15 and 19). This layer is a key bed in this area and originated from the Taisetsu-Tokachi volcanic field in central Hokkaido. Subaqueous facies of the pyroclastic flow of Ak7 can be recognized here. We can also take in a broad view of the active Me-akan volcano.

STOP 2-4: Strongly welded pyroclastic flow deposits of Ak3 and Ak4, and non-welded pyroclastic flow of Ak1 and proceeding tephra (Mosetsuri)

This is a nice outcrop of the pyroclastic flow deposits of Ak3, Ak4, and Ak7 in descending order (Figure 38). Ak3 and 4 consist of a densely welded core enclosed by partially welded material. A non-welded part at the base of Ak3 and Ak4 gradually changes into a strongly welded zone as it goes upward. This welding sequence corresponds to the cooling unit (Smith, 1960a). In this outcrop, look out for falling welded tuffs.

A thick pyroclastic flow deposit of Ak1 is also exposed here. This deposit is massive, poorly sorted, and abundant in white pumice. Several flow units (Smith, 1960b) can be recognized. Ak1 is covered by pumice falls from Me-akan and Mashu volcanoes and by fine distal ash layers from Tarumai and Komagatake volcanoes, located on the southwestern Hokkaido (in ascending order). In this location, we can also have a good view of the caldera wall and two post-caldera volcanoes of the Akan caldera.

Day 3
Me-akan trekking

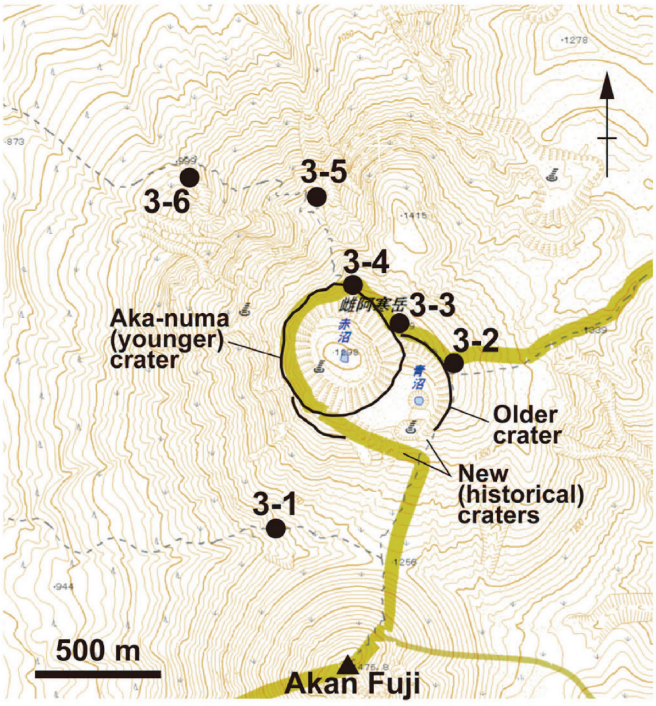

Figure 39. Locality map of stop points during Me-akan trekking (Day 3) based on parts of topographic maps from Geographical Survey Institute of Japan. Heavy lines show rims of the Older and the Younger (Aka-numa) craters.

We will climb from the On-netoh (one of the dammed lakes in the Akan caldera), across the top of the Me-akan (Ponmachineshiri), and down to a hot spring (Figure 39).

STOP 3-1. Akan Fuji

On the way to the top, we will see a young scoria cone of Akan Fuji. This volcano started its activity ca. 2.5 ka, which continued for 1.5 kyr. Its mode of eruption is mainly scoriaceous sub-plinian. Lava flows were often associated with the scoria eruption.

STOP 3-2. The older crater of Ponmachineshiri

The Ponmachineshiri crater has an oval shape (Figure 24) and a double structure composed of an older carter (ca. 0.7 ka) and the younger Aka-numa crater (ca. 0.4 ka). We can see the beautiful Ao-numa crater at the bottom of the older crater. Several new craters, such as from the 1996 and 1998 eruptions, can also be seen at the southern rim of the older crater.

STOP 3-3. The top of Ponmachineshiri

We can observe the Nakamachineshiri crater (1.1 km in diameter) from this spot. The crater was formed by two large explosive eruptions around a hundred thousand years ago (Stage II) (Figure 24). If the weather permits, we may see O-akan and Lake Akan as well. Lake Akan is famous for its spherical moss (marimo).

STOP 3-4. The younger crater of Ponmachineshiri (Aka-numa)

The deeper bottom level of Aka-numa indicates that this crater is younger than the other one. Piles of young pyroclastic ejecta covering the Ponmachineshiri lava flow can be observed here. A scoria fall from Akan Fuji is covered by scoriae and bombs from Ponmachineshiri, which are the latest magmatic eruption deposits, having occurred at approximately one thousand years ago. Several phreatic eruption deposits cover the surface of these magmatic deposits.

STOP 3-5. Northern outer wall of the Nakamachineshiri crater

From here we can observe that the summit edifice of Nakamchineshiri is covered by the large explosive eruption deposits of Stage II, which are composed of pumices, scoriae, and weakly welded pyroclastic flow deposits. We can also view the depositional surface of the pyroclastic flow. In addition, Fuppushi volcano and some lava domes can be viewed from this spot.

STOP 3-6. Internal structure of a small stratovolcano (Nishiyama)

There is a good exposure of the eruption sequence of a small basaltic stratovocano (Nishiyama: Stage III) in this location. The lower part of the outcrop consists of thick scoria falls, and the upper part is composed of at least four lava flows and agglutinate. There is no weathered layer between the parts, suggesting that the sequence was formed by a single eruption event.

We will walk on lahar deposits and lava flows from Ponmachineshiri and past some pine trees on our descent.

Day 4

Kutcharo caldera-forming eruptions

STOP 4-1: Overview of the Kutcharo caldera (Mokoto pass)

The Kutcharo caldera is the largest Quaternary caldera in Japan. Its shape has been mostly determined by the largest caldera-forming eruption Kp IV at ca. 120 ka. Two post-caldera volcanoes, Atosanupuri and Nakajima (the center of the caldera lake: Figure 26), can be clearly viewed from here.

STOP 4-2: Widespread tephra from Kyushu, southern Japan (Kamitoku)

Kp IV, Kp II/III, and Kp I are well exposed here (Figure 38). Kp III is an ash-rich pyroclastic flow deposit containing fresh andesitic lithics. There is no considerable time gap between Kp II and Kp III. Just below Kp III is a fine-ash layer composed of the co-ignimbrite ash fall deposit “Aso-4” derived in 90 ka from the Aso caldera located in central Kyushu island (about 1,500 km away from Hokkaido), southern Japan. This layer consists mainly of bubble-wall glass shards without minerals. A phreato-plinian fall deposit of Kp I can be observed here.

STOP 4-3: Successive flow units of the Kp IV eruption (Raiun)

We can see the pyroclastic flow units of Kp IV in this spot. The lower unit (Unit 3) is white and rich in lapilli pipes (Figure 28). The upper flow unit (Unit 4) is a yellowish-brown, mafic clast-rich pyroclastic flow deposit. Unit 4 covers Unit 3 conformably, with a slight erosion gap in which lapilli pipe structures of the top of Unit 3 are cut by Unit 4. This suggests that a sufficient break occurred, which allows the hot and gaseous Unit 3-U to cool down before the deposition of Unit 4. Gully channel erosion developed just after burying by Kp IV pyroclastic flow units can be observed.

STOP 4-4: Strongly welded facies of Kp IV (Sakura waterfall)

Kp IV shows thick, welded facies due to damming by the volcanic edifice of Mts. Etombi (713 m) and Shari (1547 m). The maximum thickness of the facies is more than 200 m. A waterfall (Sakura no Taki) of welded tuff presents an obstacle to salmon swimming upstream.

STOP 4-5: Atosanupuri lava dome

The Atosanupuri dome is an active dacitic lava dome, with a younger dome (west side) covering an older one (east side). Its latest phreatic explosion took place several hundred years ago. Hydrothermal alteration and sulfur deposition from fumaroles are found around the dome. Volcanic crustal deformation around the dome has also been recently observed by In-SAR.

Day 5

Mashu volcano

STOP 5-1: Overview of the Mashu caldera (Sightseeing place)

We can see the caldera of Mashu volcano from here. The Kamuinupuri cone and Kamuishu island lava dome can also be clearly observed. Older somma lava from Mashu volcano and welded Kutcharo pyroclastic flow deposits are exposed at the northern caldera wall.

STOP 5-2. Sequence of the main caldera-forming eruption in 7.5 ka (Biruwa)

The 7.5-ka eruption (Ma-mcf) was the largest caldera-forming eruption of Mashu volcano. The ejecta consisted of a plinian fall (Ma-j ~ Ma-g) and a large-scale pyroclastic flow deposit (Ma-f) (Figure 34). Lahar occurred during the eruption. We can also see a large pyroclastic flow deposit of Ch-C from Atosanupuri volcano (Figure 40). The juvenile pumices of Mashu and Atosanupuri are easily distinguishable by their vesicularity and phenocryst contents. Widespread tephras from southwestern Hokkaido, such as Ta-c (2.5 ka from Tarumai volcano), Ko-c (from the AD 1694 eruption of Komagatake volcano), and Ta-a (AD 1739), can be found in the uppermost soil layers.

STOP 5-3: Pyroclastic flow of the main caldera-forming eruption in 7.5 ka (behind Mashu station)

In this outcrop, we can observe the matrix-supported, poorly sorted, thick (> 10 m) pyroclastic flow deposit of Ma-f, which has with several flow units. The juvenile material of Ma-f varies, consisting of white pumice, light- to dark-gray pumices, and mingled pumice (Figure 34).

STOP 5-4: Products from the Kamuinupuri cone

Eruptive materials from the Central cone (Kamuinupuri) formation are exposed at this outcrop, 6 km ENE of Kamuinupuri volcano (Figure 40). Ma-e is an ash layer at 5.5 ka. Ma-d (4.0 ka) changes from an lithic-rich ash fall to a coarser pumice fall deposit in ascending order. Ma-c (1.7 ka) is subdivided into Ma-c1 ~ c4 by intervening thin soil layers.

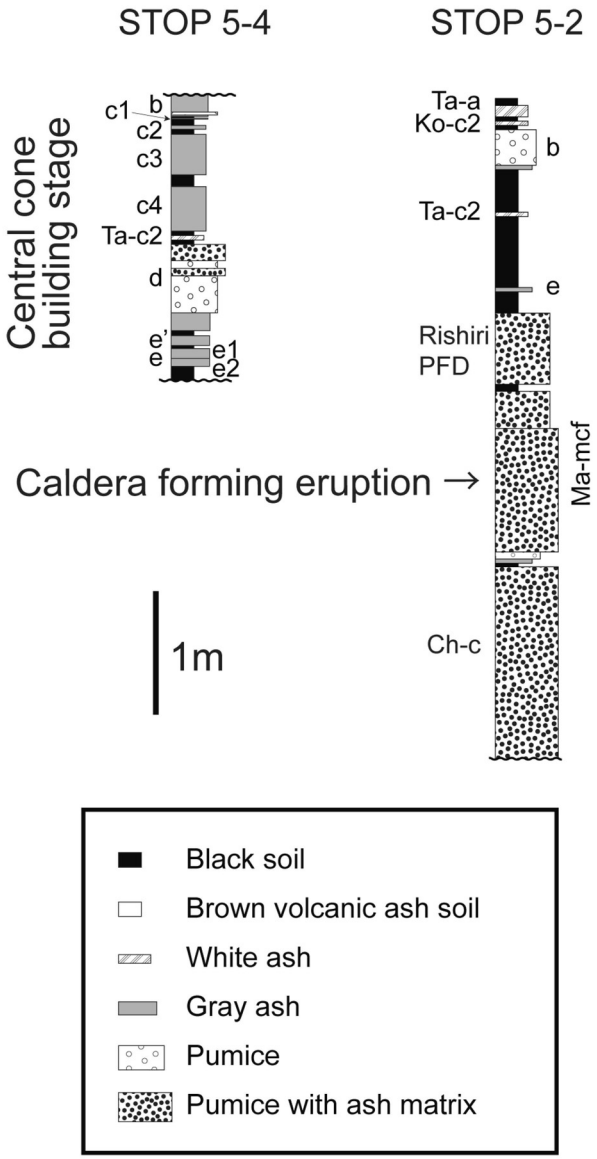

Figure 40. Geological columns of STOP 5-2 and 5-4. Ma-b ~ Ma-e are abbreviated as "b ~ e". Rishiri PFD is a small pyroclastic flow deposit (ca. 5.5 ka) from Rishiri dome on the southwest of Atosanupuri dome (see Figure 32).

Ta-c of 2.5 ka can be found between Ma-d and Ma-c. Ma-b is not well observed here because its main axis is directed to the north. The eruptions during the central cone formation were characterized by activity shifts from the phreatic to the magmatic phase.

STOP 5-5: Low-K tholeiitic basalt scoria cone

A small scoria cone (40 m in height) is located 10 km SE of Mashu volcano. This cone is one of the satellite vents of Mashu volcano and forms the NW-SE trend with

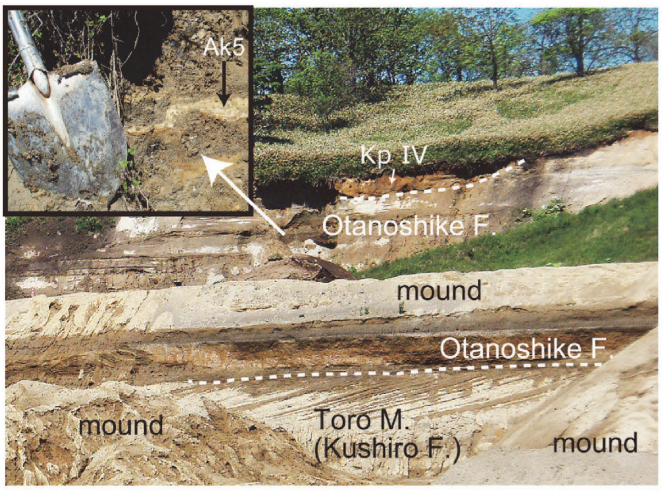

Figure 41. An outcrop photograph. Lowermost Toro Member (M.), greater than 10 m in thickness, showing remarkable cross-stratification. Inset is a close-up of the Ak5 tephra, with spade for scale. F., Formation.

Kamuinupuri volcano and Mt. Nishibetsu-dake. The ejecta of this cone consists of tholeiitic basalt with extremely low K_2O content. The scoria cone is covered by Ma-mcf eruption deposits, but its detailed age has not been determined.

Day 6

6-1: Pyroclastic materials in marine deposits (behind Kushiro National College of Technology)

We can observe pyroclastic materials and key tephra beds in the Quaternary terrigenous marine deposits (Kushiro, Toro and Otanoshike Formations) in this region (Figure 41). The detailed identification of these pyroclastic materials is based on the stratigraphy, glass chemistry, contents, and assemblages of phenocrysts. The identification of the tephras (eg., Ak5 and Kp IV) helps us to determine the ages of the marine sediments and related transgression.

Summary:

Hokkaido is situated at the junction of two arc-trench systems, the NE Japan and Kuril arcs, both of which have experienced intense volcanism since late Miocene. We will visit central and eastern Hokkaido, where locates at the southern end of the Kuril arc. We will focus on various types of younger volcanoes, calderas (Akan, Kutcharo and Mashu), a volcanic complex (Taisetsu-Tokachi volcano group), and post-caldera volcanoes (Me-Akan and Atosanupuri). These volcanoes have erupted tephra deposits that are widely distributed in Hokkaido. We will investigate these deposits to reconstruct the eruption sequences and magmatic processes. In addition, we will climb Tokachi-dake and Me-Akan volcanoes to investigate their respective structures. We will also focus on the snow-melt lahar associated with the AD 1926 eruption of Tokachi-dake volcano, which caused severe hazards and killed 144 people.

Acknowledgments

We are grateful to two reviewers, Professor Masashi Tsukui (Chiba University) and Professor Takeshi Kuritani (Osaka City University).

References

Carey, S. and Sparks, R.S.J. (1986) Quantitative models of the fallout and dispersal of tephra from volcanic eruption columns, Bulletin of Volcanology, 48, 109–125.

Chapman, M.E. and Solomon, S.C. (1976) North American-Eurasia plate boundary in northeast Asia. Jour. Geophys. Res., 81, 921-930.

Fujiwara, S., Nakagawa, M., Hasegawa, S. and Komatsu, D. (2007) Eruptive History of Tokachi-dake Volcano during the Last 3,300 Years, Central Hokkaido, Japan, Bull. Volcanol. Soc. Japan, 52, 253-271 (in Japanese with English Abstract).

Fujiwara, S., Ishiduka, Y. Yamazaki, T. and Nakagawa, M. (2009) Newly Found . ka Pyroclastic Flow Deposits on the Northwestern Foot of Tokachi-dake Volcano, Central Hokkaido, Japan and Reexamination of the Eruptive Activity During Holocene. 6, 253-262 (in Japanese with English Abstract).

Gill, J. B. (1981) Orogenic andesites and plate tectonics. Splinger-Verlag, Berlin-Hetelberg, New York, 385p.

Gnibidenko, H.S., Hilde, T.W.C., Gretskaya, E.V. and Andreyev, A.A. (1995) Kuril (South Okhotsk) backarc basin. In backarc basins, tectonics and magmatism, Taylor, B. editor, Plenum Press, New York and London, 421-449.

Goto, Y., Funayama, A., Gouchi, N. and Itaya,T. (2000) K-Ar ages of the Akan-Shiretoko volcanic chain lying oblique to the Kurile

trench: Implications for the tectonic control of volcanism, Island Arc, 9, 204-218.
Hasegawa, T., Ishii, E. and Nakagawa, M. (2006) Evolution of Akan Caldera, East Hokkaido, indicated by analysis of lithic fragments in pumice fall deposits (in Japanese), The Earth Monthly, 28, 283-289.
Hasegawa, T. and Nakagawa M. (2007), Stratigraphy of Early to Middle Pleistocene pyroclastic deposits around Akan caldera, eastern Hokkaido, Japan, J. Geol. Soc. Jpn, 113, 53-72 (in Japanese with English abstract).
Hasegawa, T., Ishii, E. and Nakagawa, M. (2008) Correlations of distal ash layers in the Akan pyroclastic deposits, eastern Hokkaido, with large-scale pyroclastic flow deposits distributed in central Hokkaido, Japan. J. Geol. Soc. Jpn, 114 , 366-381 (in Japanese with English abstract).
Hasegawa, T., Yamamoto, A., Kamiyama H. and Nakagawa M. (2009a) Gravity structure of Akan composite caldera, eastern Hokkaido, Japan: Application of lake water corrections, Earth Planets and Space, 61, 933-938.
Hasegawa, T., Kishimoto, H., Nakagawa, M., Itoh, J., Yamamoto, T., (2009b) Eruptive history of post-caldera volcanoes of Kutcharo caldera, eastern Hokkaido, Japan, as inferred from tephrostratigraphy in the Konsen and Shari areas for the period 35-12 ka, J. Geol. Soc. Japan, 115, 369-390 (in Japanese with English abstract).
Hasegawa, T., Nakagawa, M., Itoh, J. and Yamamoto, T. (2011) Deposition ages of Quaternary sequences in Kushiro region, eastern Hokkaido, Japan: Correlations and chronology on the basis of high-resolution tephro-stratigraphy, J. Geol. Soc. Jpn., (in Japanese with English abstract).
Hasegawa, T., Nakagawa, M. and Kishimoto, H. (2012) The eruption history and silicic magma systems of caldera-forming eruptions in eastern Hokkaido, Japan. Journal of Mineralogical and Petrological Sciences, 107, 39-43.
Hirose, W. and Nakagawa, M. (1995) K-Ar ages of the Neogene volcanic rocks from the Kutcharo caldera region, east Hokkaido, with special reference to the Quaternary volcanic history. J. Geological Society of Japan, 101, 99-102 (In Japanese with English Abstract).
Hirose, W. and Nakagawa, M. (1999) Neogene volcanism in Central-Eastern Hokkaido: Beginning and evolution of arc volcanism inferred from volcanological parameters and geochemistry. Jour. Geol. Soc. Japan, 105, 247-265. (in Japanese with English abstract)
Hirose, W., Iwasaki, M., and Nakagawa, M. (2000) Transition of Neogene arc volcanism in Central-Western Hokkaido, viewed from K-Ar ages, style of volcanic activity, and bulk rock chemistry. Jour. Geol. Soc. Japan, 106, 120-135 (in Japanese with English abstract).
Hirose, W., Okazaki, N., Ishimaru, S., Hasegawa, T., Fujiwara, S., Nakagawa, M., Sasaki, H., Sato, J. Sapporo District Meteorological Observatory and Kushiro Local Meteorological Observatory (2007) The eruption on March 2006 at Meakandake Volcano, Hokkaido, northern Japan: eruption process and ash fall survey. Report of the Geological Survey of Hokkaido, 78, 37-55 (in Japanese with English abstract).
Ichihara, H., Mogi, T. Hase, H. Watanabe T. and Yamaya Y. (2009) Resistivity and density modelling in the 1938 Kutcharo earthquake source area along a large caldera boundary. Earth Planets and Space, 61, 345-356.
Ikeda, Y., and Mukoyama, S., (1983) Stratigraphy and correlation of the pyroclastic flow deposits in the Furano-Asahikawa area, central Hokkaido, Japan. J. Geol. Soc. Japan, 89, 163-172 (in Japanese with English abstract).
Ishii, E., Nakagawa, M., Saito, H. and Yamamoto, A. (2008) The Pleistocene Tokachimitsumata caldera and associated pyroclastic flow deposits in central Hokkaido, Japan: Correlation of large scale pyroclastic flow deposits with source calderas. J. Geol. Soc. Jpn, 114, 348-365 (in Japanese with English Abstract).
Ishikawa, T., Yokoyama, I., and Katsui, Y. (1972) Tarumai-san, the report on the volcanoes of Hokkaido. Committee for prevention of the natural disaster of Hokkaido, 124p. (in Japanese)
Ishikawa, T., Yokoyama, I., Katsui, Y. and Kasahara, M. (1971) Tokachi-dake, its volcanic geology, history of eruption, present state of activity and prevention of disasters. Committee for prevention of the natural disaster of Hokkaido, 136p (in Japanese).
Itoh, H., Ozeki, N., Makinou, T. and Anyoji, N. (1997) Tephrochronogical Study in the Eastern region of the Tokachidake Volcano, 1997 Fall Meet. Volcanol. Soc. Japan, Abstr., 4 (in Japanese).
Japan Meteorological Agency (JMA) (2005) National Catalogue of the Active Volcanoes in Japan, third edition. 635p.

Katsui, Y. (1958) Akan and Kutcharo volcanoes. Earth Science, 39, 19-29 (In Japanese).

Katsui, Y and Satoh, H.R. (1963) Explanatory text of the geological map of Japan, scale 1: 50,000, Mokoto-yama. pp.42, Hokkaido Development Agency, Sapporo (In Japanese with English Abstract).

Katsui, Y. and Ishikawa, T. (1981) The eruptive history, its ejecta, disaster map and evaluation of hazard on the Tarumai-san. Report on the characteristics hazard mapping, and forecasting of eruptive hazards, Research project of natural disaster, the Ministry of education, science, and culture of Japan. 9-13. (in Japanese)

Katsui, Y., Suzuki, T., Soya, T. and Yoshihisa, Y. (1989) Geological map of Hakkaido-Komagadake Volcano 1 : 50,000 Geological map of volcano 5. Geol. Surv. Japan, 10 p (in Japanese with English abstract).Katsui, Y., Kawachi, S., Kondo, Y., Ikeda, Y., Nakagawa, M., Gotoh, and Y., Yamagishi, H (1990) The 1988-1989 explosive eruption of Tokachi-dake, Central Hokkaido, its sequence and mode. Bull. Volcanol. Soc. Japan, 35, 111-129.

Kiminami., K., Kawamura, N., Niida, K., Watanabe, T. and Kato, M. (1990) Tectonic divisions of Paleozoic and Mesozoic rocks of Hokkaido. in Geology of Japan. (Kato, N. et al. ed.), Terra, Tokyo, 117-128.

Kimura, G. (1986) Oblique subduction and collision: Forearc tectonics of the Kuril Arc. Geology, 14, 404-407.

Kishimoto, H., Hasegawa, T., Nakagawa, M. and Wada, K. (2009) Tephrostratigraphy and eruption style of Mashu volcano, during the last 14,000 years, eastern Hokkaido, Japan. Bull. Volcanol. Soc. Japan, 54, 15-36. (in Japanese with English abstract).

Machida, H., and Arai, F. (2003) Atlas of Tephra in and around Japan. pp. 336, Tokyo University Press (in Japanese).

Matsui, M., Matsuzawa, I. and Yamaguchi, S. (1970) On the Osarushinai Foramation- Early Pleistocene Deposits of Tokachi Plain, Hokkaido, Quatern. Res., 9, 123-127 (in Japanese with English Abstract).

Nakagawa, M. (1999) Origin of spatial compositional variations in differentiated arc volcanics at arc-arc junctions: A case study of major and trace element variations in Quaternary volcanics from Hokkaido, Japan. Resource Geology Special Issue, 20, 161-176.

Nakagawa, M., Maruyama, H., Funayama, A. (1995) Distribution and spatial variation in major element chemistry of Quaternary volcanoes in Hokkaido, Japan. Bull. Volcanol. Soc. Japan, 40, 13-31. (in Japanese with English abstract)

Nakamura, K. (1983) Possibility of nascent plate boundary at the eastern margin of the Japan sea. Bull. Earthquake Res. Inst., Univ. Tokyo, 58, 711-722

NEDO (1990) Report on the distribution and geochronology of volcanic rocks, fiscal year 1989 of nationwide “Tokachi district”. 456p (in Japanease).

NEDO (1992) Report of Geothermal development promotion survey, Akan area., New Energy and Industrial Technology Development Organization. 26. pp 1133, (in Japanese).

Okamura, Y., Watanabe, M., Morijiri, R. and Satoh, M. (1995) Rifting and basin inversion in the eastern margin of the Japan Sea. The Island Arc, 4, 166-181.

Sagawa, A., Shibata, K., Yamagachi, S. and Hasaka, T. (1984) Paleomagnetism and K-Ar age of pyroclastic rocks on the upper stream area of the Tokachigawa river, Hokkaido. Bull. Geol. Surv. Japan, 35, 365-381 (In Japanese with English Abstract).

Satoh, H.R. (1965) Explanatory text of the geological map of Japan, scale 1: 50,000, Akanko. pp.82, Geological Survey of Japan (In Japanese with English Abstract).

Seno, T. (1985) Is northern Honshu a microplate? Tectonophysics, 115, 177-196.

Smith, R. L. (1960a) Zones and zonal variations in welded ash-flows. U. S. Geological Survey Professional Paper, 354-F, 149-159.

Smith, R. L. (1960b) Ash flows. Geol. Soc. Amer. Bull. 71, 795-842.

Sumita, M. (2003) Kutcharo caldera and ignimbrite, In Regional Geomorphology of the Japanese Islands. Vol. 2. Geomorphology of Hokkaido (Koaze, T., Nogami, M., Ono, Y. and Hirakawa, K. eds), University of Tokyo Press, 110-111 (in Japanese).

Tamada, J. and Nakagawa, M. (2009) Eruption History of Oakan Volcano, Eastern Hokkaido, Japan. Bull. Volcanol. Soc. Japan, 54, 147-162.

Tamaki, K. (1995) Opening tectonics of the Japan sea., in Back-arc basins-tectonics and magmatism. (Taylor, B. ed.) Plenum Press., New York and London, 407-420

Tokuda, S. (1926) On the echelon structure of the Japanese archipelagoes. Japanese J. Geology

and Geography, 5, 41-76.
Uesawa, S. (2008) Restudy of Stratigraphy and Paleomagnetic Characteristics of Taisho Lahar Deposit Associated with the 1926 Eruption on Tokachidake Volcano, Central Hokkaido, Japan. Bull. Volcanol. Soc. Japan, 53, 171-191 (in Japanese with English Abstract).
Wada, K. (1989) Mixing Mechanism of Heterogeneous Magmas at the Somma-building Stage of Meakan Volcano, Eastern Hokkaido, Japan. Bull. Volc. Soc. Japan, 34, 89-104 (in Japanese with English Abstract).
Wada, K. (1991) Mixing and Evolution of Magmas at Me-Akan Volcano, Eastern Hokkaido, Japan. Bull. Volc. Soc. Japan, 36, 61-78 (in Japanese with English Abstract).
Wada, K. (1995) Fractal structure of heterogeneous ejecta from the Me-akan volcano, eastern Hokkaido, Japan: implications for mixing mechanism in the volcanic conduit. J. Volcanol. Geotherm. Res., 66, 69-79.
Wohletz, K.H.（1983) Mechanisms of hydrovolcanic pyroclastic formation: grain-size, scanning electron microscopy, and experimental studies. J. Volcanol. Geotherm. Res., 17, 31-63.
Yahata, M. (1989) The Kutcharo Caldera －A Consideration on the Relationship between the Basement Structure and the Formation of Caldera－. Monogr. Assoc. Geol. Collab. Japan, 36 , 191-208. (in Japanese with English abstract).
Yamamoto, T., Itoh, J., Nakagawa, M., Hasegawa, T. and Kishimoto, H. (2010) ^{14}C ages for the ejecta from Kutcharo and Mashu calderas, eastern Hokkaido, Japan. Bull. Geol. Surv. Japan, 61, 161-170 (in Japanese with English Abstract).
Yokoyama, I., Katsui, Y., Ehara, S., and Koide, K. (1976) Meakandake, its volcanic geology, history of eruption, present state of activity and prevention of disasters. Committee for Prevention of Disasters of Hokkaido, 138p (In Japanese).

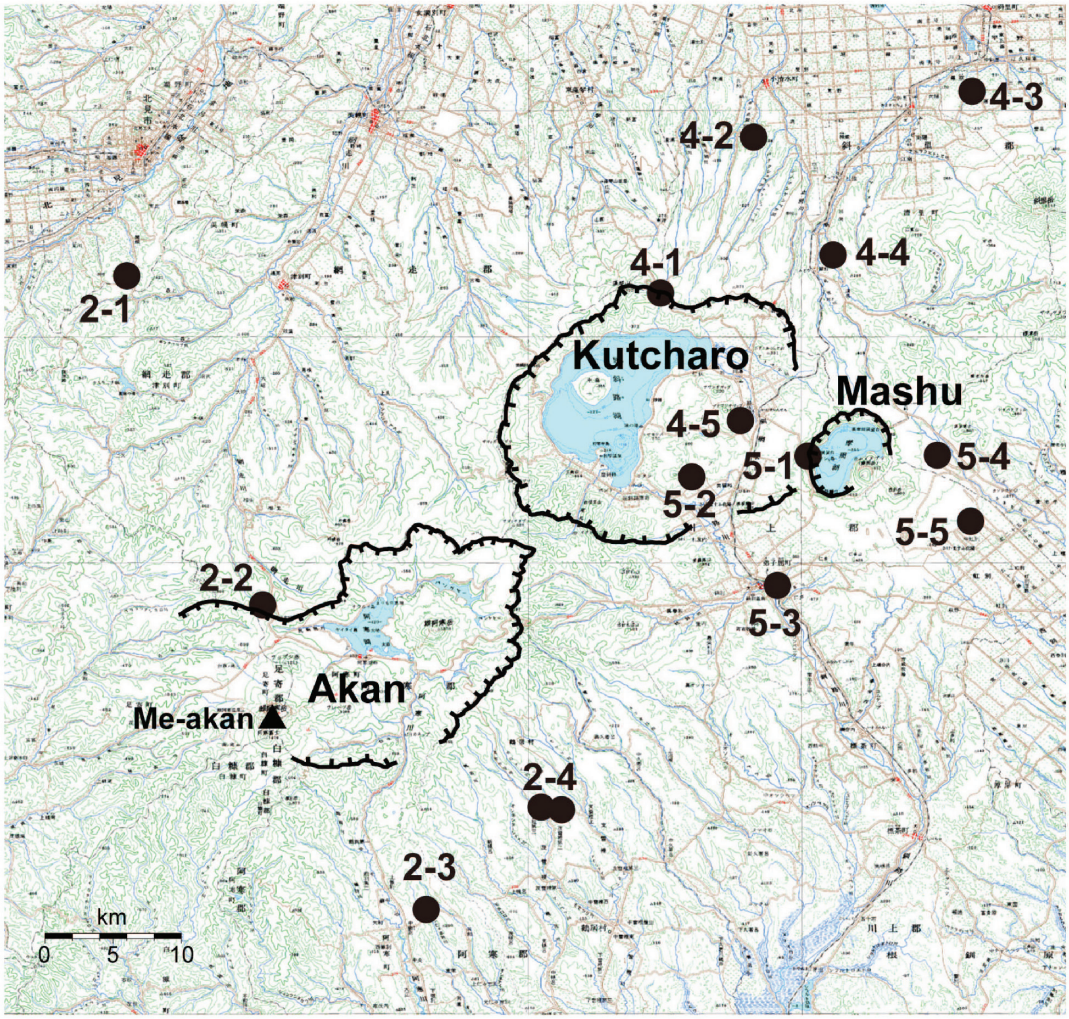

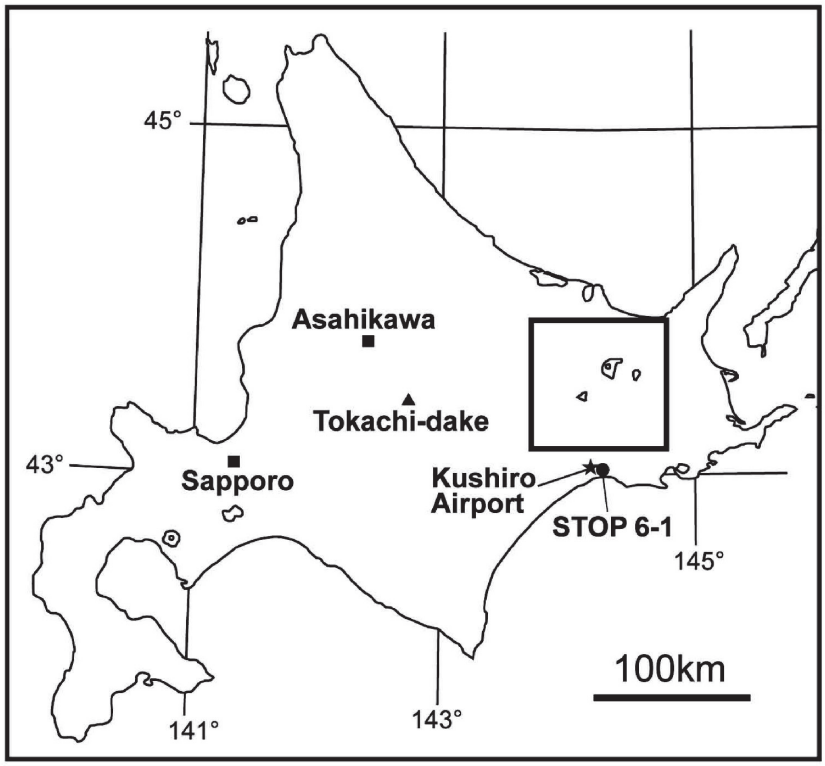

Appendix. Maps showing stops (circles) and towns (squares) of Hokkaido field trip based on parts of topographic maps from Geographical Survey Institute of Japan. A box in the lower (Hokkaido island) map encloses an area of upper map. Heavy lines of upper map indicate caldera rims of Akan, Kutcharo and Mahu volcanoes.